Provided for non-commercial research and educational use only.
Not for reproduction, distribution or commercial use.

This chapter was originally published in the book *Developments in Soil Science, Vol. 34,* published by Elsevier B.V., and the attached copy is provided by Elsevier for the author's benefit and for the benefit of the author's institution, for non-commercial research and educational use including without limitation use in instruction at your institution, sending it to specific colleagues who know you, and providing a copy to your institution's administrator.

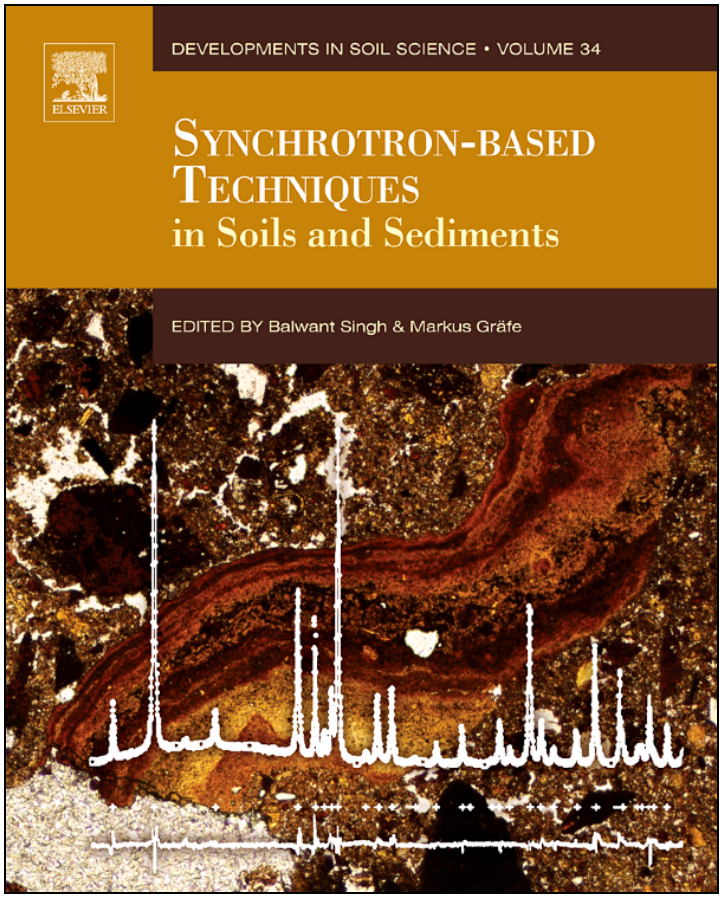
DEVELOPMENTS IN SOIL SCIENCE • VOLUME 34
ELSEVIER
SYNCHROTRON-BASED TECHNIQUES in Soils and Sediments
EDITED BY Balwant Singh & Markus Gräfe

All other uses, reproduction and distribution, including without limitation commercial reprints, selling or licensing copies or access, or posting on open internet sites, your personal or institution's website or repository, are prohibited. For exceptions, permission may be sought for such use through Elsevier's permissions site at:
http://www.elsevier.com/locate/permissionusematerial

From: Theodore K. Raab and David A. Lipson, The Rhizosphere: A Synchrotron-Based View of Nutrient Flow in the Root Zone. In Balwant Singh and Markus Gräfe: Developments in Soil Science, Vol. 34. Elsevier B.V., The Netherlands, 2010, pp. 171-198.
ISBN: 978-0-44-453261-9
© Copyright 2010, Elsevier B.V.
The Netherlands

Author's personal copy

CHAPTER

7

The Rhizosphere: A Synchrotron-Based View of Nutrient Flow in the Root Zone

Theodore K. Raab[1] *and David A. Lipson*[2]

[1]Stanford University, Department of Biology, Stanford, CA, USA
[2]San Diego State University, Department of Biology, San Diego, CA, USA

OUTLINE

1. Introduction 171
2. Effects of Plant Roots on the Rhizosphere Microenvironment 172
3. Plant-Microbe Interactions in the Rhizosphere 173
4. Questions Amenable to Synchrotron-Based Imaging Methods: Opportunities and Challenges 175
5. Synchrotron IR Microscopy: Establishing Models for Rhizosphere Interactions 176
6. Characterizing and Improving Rhizobox Technology: IR Optics Issues 179
7. Plant-Culture Issues 180
8. Polyuronic Acids in Root Mucilage 184
9. Scanning Transmission X-Ray Microscopy Applications in Ecology 187
10. Conclusions 192

1. INTRODUCTION

Surface polysaccharides and exudates of plants are often the first point of contact between foreign organisms and plants, in addition to acting as mechanical scaffolding to support land plants, or simple stored energy sources. The ecological role of these polysaccharides can be both positive and negative, and in this review, we consider both

Copyright © 2010, Elsevier B.V.
All rights reserved.

Author's personal copy

aspects, especially as revealed through the use of synchrotron-based IR spectroscopy. We briefly review the microbiological characteristics of rhizosphere-associated microorganisms, interactions with plant growth, and some of the recent chemical communication pathways (Quorum Sensing/quenching) identified in the soil. From the plant perspective, recent work in model genetic systems points to two mechanisms whereby low-molecular-weight natural compounds may be excreted into the root environment in response to pathogen attack or abiotic stress (Hückelhoven, 2007; Loyola-Vargas et al., 2007). *Exocytosis* through the plant endomembrane system, or direct, energized transport through ATP-binding cassette (ABC) transporter proteins of the root plasma membrane (Loyola-Vargas et al., 2007; Stein et al., 2006) are two conceivably nonoverlapping, nonexclusive pathways for plants to regulate the chemistry of the near-root environment. Using synchrotron IR microscopy (SIRM) and nonmodel system plants from among legumes, mustards and ferns, we find that an important fraction of the fixed carbon entering the rhizosphere imparts a characteristic physical coherence to the soil over spatial scales of 40-140 μm through highly charged polysaccharide polymers, and to a lesser extent, proteins. Though classical biochemical methods provide much information on the average chemical composition of these exopolysaccharides (EPS), it is precisely the spatial context of the exudates that are the point of much rhizosphere research. The acidity and ion exchange behavior of these EPS almost certainly result in rates of chemical weathering of soil minerals far in excess of what might result from "neutral" polymers. At the very end of this chapter, we discuss recent experiments using soft X-ray microscopy to study nutrient transfer from plant litter.

2. EFFECTS OF PLANT ROOTS ON THE RHIZOSPHERE MICROENVIRONMENT

By definition, the soil in the rhizosphere is altered by the presence of plant roots. Roots alter their environment by absorbing nutrients, exchanging gases, and exuding organic compounds. Roots effectively deplete nutrients in their immediate vicinity by active uptake (see reviews by Cardon and Gage, 2006; Hinsinger et al., 2005; Kuzyakov, 2002; Raab et al., 1999; Somers et al., 2004). The absorption of charged molecules by roots can also alter the pH of the rhizosphere, as they may release either protons or bicarbonate ions to maintain charge balance, while taking up cations or anions, respectively. Respiration by roots and their associated microbial communities can increase CO_2 in the soil atmosphere by two orders of magnitude, while simultaneously lowering O_2 concentrations. However, in waterlogged soils, aerenchymous plants channel gases between the soil and the atmosphere, leading to increased O_2 availability in the rhizosphere relative to the anaerobic bulk soil. Plant roots contribute a wide variety of organic compounds to the soil through active and passive processes. These compounds have been classified as *exudates* (simple compounds passively leaking across the membranes of live plant cells), *secretions* (actively released substances, such as enzymes or ligands), *mucilage* (complex polymeric substances released by root cells or by the sloughing of the root cap), and *lysates* (compounds liberated from root cells during microbial degradation) (Kuzyakov, 2002; Somers et al., 2004). These effects lead to specialized microbial communities that further alter the rhizosphere. For example, biofilms on root surfaces produce a matrix of extracellular polymeric substances (EPS), which, together with plant-produced mucilage and the physical

Author's personal copy

compaction effects of growing roots, alter the soil structure within the rhizosphere (Feeney et al., 2006; Hinsinger et al., 2005; Raab and Vogel, 2004). Similarly, *glomalin*, a glycoprotein produced by arbuscular mycorrhizal (AM) fungi of the genus *Glomus*, effectively binds soil into microaggregates (Rillig and Steinberg, 2002). Improved structure of the soil increases the size of soil pores, leading to enhanced diffusion of gases and altered water holding properties of the soil. While the rhizosphere has been defined in diverse ways, many studies employ a simple operational definition by sampling the soil that clings to plant roots (Hinsinger et al., 2005). This definition, besides being experimentally convenient, is consistent with the rhizosphere being the zone of immediate influence of roots, at least with respect to EPS production.

3. PLANT-MICROBE INTERACTIONS IN THE RHIZOSPHERE

The rhizosphere is a thriving metropolis where plant roots, mycorrhizal fungi, and diverse microbial populations, both beneficial and harmful, intersect. The interrelationships among these players are accordingly complex, and, just as plant roots profoundly alter the microhabitat experienced by microbes, rhizosphere communities can be powerful drivers of plant processes (van der Heijden et al., 2008). It has long been hypothesized that the release of organic compounds by roots into the rhizosphere can stimulate nutrient cycling through a "priming effect" on soil microbes (Clarholm, 1985; Finzi et al., 2007; Herman et al., 2006; Kuzyakov, 2002; Raynaud et al., 2006, 2008; Saj et al., 2007). The input of C from roots stimulates microbes, which produce extracellular enzymes that release nutrients from complex soil organic matter (OM). These nutrients are eventually released from microbial biomass by predation (Clarholm, 1985; Ingham et al., 1986), natural dynamics of root growth (Darrah, 1991), or seasonal fluctuations in microbial biomass (Lipson et al., 1999; Singh et al., 1989). Many studies support this general model, though there is a broad diversity of specific results: some studies find elevated microbial biomass in the rhizosphere (Phillips and Fahey, 2006), others find little or none (Herman et al., 2006); elevated populations of microbial grazers have been observed in some cases (Clarholm, 1985), but not in others (Herman et al., 2006). In general, elevated rhizodeposition seems to increase nutrient availability (Finzi et al., 2007; Kuzyakov, 2002); however, the amount of root exudation by a plant species is not always a good predictor of its ability to acquire nitrogen (Saj et al., 2007). Furthermore, the mechanisms of enhanced rhizosphere nutrient cycling are not always clear; turnover of microbial biomass-N sometimes fails to account for the observed increase in mineralization (Herman et al., 2006). In addition, the role of bacteriophage as microbial predators in the rhizosphere has been generally overlooked (Ghosh et al., 2008).

In addition to the general lot of microbes that accelerate mineralization of nutrients from soil OM, the rhizosphere hosts a variety of beneficial microbial communities. Perhaps the most ubiquitous mutualists in the rhizosphere are mycorrhizal fungi. Mycorrhizal hyphae can be considered an extension of the root system, and it has long been observed that bacterial communities in the "mycorrhizosphere" were distinct from those in the bulk soil (Katznelson et al., 1962). Determining the extent of mycorrhizal hyphae in the soil is difficult, further complicating a precise delineation of the rhizosphere. Estimates of ectomycorrhizal hyphal length range from 100-8000 cm per cm root length (Jones et al., 1990; Read and Boyd, 1986; Rousseau et al., 1994), implying a potentially vast

Author's personal copy

mycorrhizosphere. Synchrotron studies with isolated fungi are new (Kaminsky et al., 2008), and if performed on genetically tractable organism, offer the possibility of providing functional insights into the ever present "genes of unknown function."

Much attention has been focused on plant growth promoting rhizobacteria (PGPR), such as N-fixing species of *Azospirillum* that associate with the roots of wheat, corn and other plants (Ryan et al., 2008). Associative N fixers are differentiated from mutualistic N fixers, like *Rhizobia*-Legume symbioses, in part because they do not bring about morphological changes in root growth. However, these associations involve fairly complex plant-microbe interactions, such as chemotaxis and selective binding of bacteria to root surfaces, biofilm initiation, and production of plant hormones by bacteria. Besides providing nutrients to plants, PGPR such as *Azospirillum, Pseudomonas fluorescens,* and *Agrobacterium rhizogenes* can protect plant roots from soil-borne disease by avirulently occupying the rhizosphere niche, inducing plant systemic resistance, and in some cases secreting antimicrobial compounds (Pieterse and Dicke, 2007; Ryan et al., 2008; Somers et al., 2004). Numerous symbiotic fungi, such as *Trichoderma*, carry out similar functions (Vinale et al., 2008).

Given the complex interactions among plant roots and mutualistic, commensal, and pathogenic rhizosphere microbes, it follows that the rhizosphere resounds with a cacophony of chemical signals (Bais et al., 2006). Information is transmitted by secretion of diverse compounds mediating biofilm formation, infection of roots, and modulation of plant immune response pathways. Likewise, misinformation is spread among competing populations of bacteria, by pathogenic microbes interfering with host defense signaling, and possibly by plant roots to disrupt biofilm formation or root colonization by harmful microbes (Barnard et al., 2007; Holtsmark et al., 2007; Hückelhoven, 2007; Morris and Monier, 2003; Pieterse and Dicke, 2007; Ryan et al., 2008; Somers et al., 2004; Vinale et al., 2008; Williams, 2007). Bacteria use quorum sensing (QS) to regulate gene expression in response to their population size. Each member of the population constitutively secretes a signaling molecule, which builds up in the environment, eventually reaches some threshold concentration, and activates genes for such functions as bioluminescence, virulence, or biofilm formation. A wide variety of QS signaling molecules have been described. These include peptides (generally 5-20 amino acids in length), acylhomoserine lactones (AHLs), alkylquinolones, a group of furanones referred to as autoinducer-2 (AI-2), and diverse others (Chen et al., 2002; Williams, 2007). Some of these signals appear to be species-specific, while some are sensed more generally, allowing communication between bacterial species. In fact, plants can recognize bacterial signals, and thereby alter their gene expression in response to the presence of specific species of bacteria (Mathesius et al., 2003). Conversely, rhizosphere bacteria respond to a variety of plant-produced signals, such as salicylic acid (Yuan et al., 2007), and it has been proposed that the plant hormone, indole acetic acid (IAA), may act as a QS signal in bacteria (Lambrecht et al., 2000). *Rhizobia* show chemotactic responses to nanomolar concentrations of legume-produced phenolics (Somers et al., 2004). Furthermore, many rhizosphere bacteria manufacture plant hormones (Pieterse and Dicke, 2007; Ryan et al., 2008), and some plants produce analogs of AHLs (Somers et al., 2004; Teplitski et al., 2000). Competing bacterial species produce enzymes, such as AHL-degrading lactonases, that degrade each other's QS signals (Somers et al., 2004). Despite the number of published studies, the full extent and complexity of communication among the many inhabitants of the rhizosphere is still only partially understood.

Author's personal copy

4. QUESTIONS AMENABLE TO SYNCHROTRON-BASED IMAGING METHODS: OPPORTUNITIES AND CHALLENGES

Recent reviews highlight several key gaps in knowledge about the rhizosphere: (1) how to define the boundary of the rhizosphere in terms of its many effects on soil processes and communities (Hinsinger et al., 2005); (2) how plant roots affect rhizosphere community composition, activity, and nutrient cycling (Cardon and Gage, 2006); and (3) how rhizosphere effects are modified by elevated CO_2 and climate change (Finzi et al., 2007). Questions about the rhizosphere, of both a fundamental and a detailed mechanistic nature, remain unanswered. Because of the chemical and fine-scale spatial complexity around roots, rhizosphere studies will likely benefit from synchrotron-based techniques with a spatial resolution of tens of nanometers, appropriate for nearly-hydrated samples that impart as little radiation-damage to samples as practical; in this case, soft X-ray imaging methods (Hitchcock et al., 2005; Jacobsen et al., 1991, 2000) such as scanning transmission X-ray microscopy (STXM) are appropriate (Fig. 7.1). Thus far, very few studies have taken advantage of STXM to investigate the rhizosphere. However, STXM and related methods have been used to study the fine scale distribution of various classes of organic-C and other elements within bacterial biofilms (Dynes et al., 2006; Lawrence et al., 2003; Toner et al., 2005), bacteria-soil mineral interfaces (Benzerara et al., 2005) and soil microaggregates (Kinyangi et al., 2006; Schumacher et al., 2005; Wan et al., 2007). These studies demonstrate that STXM can be applied to measuring biologically relevant data in soil microenvironments. The ability to sense multiple elements and forms of organic-C should make STXM a natural choice for determining: (1) the specific chemical signature of the rhizosphere, (2) the spatial extent of the influence of plant roots, and (3) how the geometry and chemical nature of the rhizosphere varies longitudinally from the growing root tip to the older portions of the root. Besides answering the philosophical question, "How big is the rhizosphere?" defining the spatial extent of the rhizosphere in terms of depletion profiles of nutrients will provide experimental data needed to validate models that scale from the individual root to the whole plant (Darrah et al., 2006). We will discuss our preliminary applications of STXM to microorganisms decomposing plant litter in the final section of this chapter.

As a practical application of the method, it can be seen that one of the most consistent effects of elevated atmospheric CO_2 on plants in natural ecosystems is an increased allocation of C belowground, in the form of root production and/or exudation (Hungate et al., 1997; Lipson et al., 2005). However it is still uncertain how elevated CO_2 and altered climate affect root turnover and rhizosphere processes (Finzi et al., 2007; Gill and Jackson, 2000). Mancosky et al. (2005) use STXM and Near Edge X-ray absorption fine structure (NEXAFS) to detect

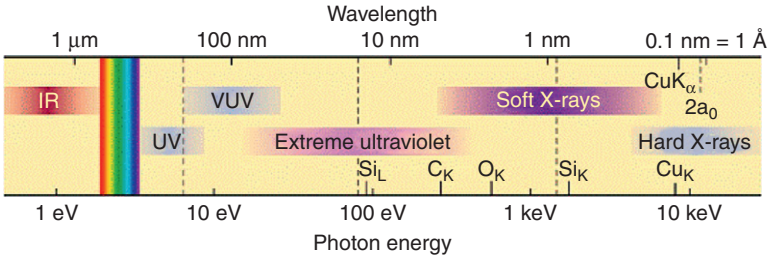

FIGURE 7.1 Graphical representation of the electromagnetic spectrum available to synchrotron radiation sources. This chapter considers the thermal IR (3–20 μm wavelength) and soft X-ray (10–30 nm wavelength) regions.

Author's personal copy

oxidative damage of lignocellulosic materials produced in a bleaching process. Is it possible that a similar analysis could be applied to quantifying the degradation of plant cell walls in studies of fine root turnover? Apart from having profound importance in terms of global change, the effects of elevated CO_2 on rhizodeposition could also serve as a practical tool for understanding the effects of roots on the soil environment: elevated CO_2 allows a manipulation of the spatial extent of the rhizosphere.

5. SYNCHROTRON IR MICROSCOPY: ESTABLISHING MODELS FOR RHIZOSPHERE INTERACTIONS

Why do we need a synchrotron for our proposed studies? The improvement in imaging technology described in this chapter rests in the ability to use the mid-IR spectroscopic signatures of organic and inorganic compounds as *noninvasive contrast reagents* for microscopic examination (and mapping) of the root zone. Such examination became possible in the mid-1990s (Carr, 1999; Carr et al., 1995; Jamin et al., 1998; Martin and McKinney, 1998) with the advent of high-brightness IR synchrotron radiation sources, as they exist now in the United States at the Brookhaven National Labs (NSLS, NY), Lawrence Berkeley National Lab (ALS, CA), the Synchrotron Radiation Center in Wisconsin (SRC, WI), and the Center for Advanced Materials and Devices (CAMD, LA), with most of the large electron-storage rings in the multi-GeV energy range developed as user facilities by the US Department of Energy. Facilities are also in operation/under construction in Europe, Canada and Australia, with Diamond in the UK, BESSY2 in Berlin, Soleil in France, MAXLAB in Sweden, the CLS in Canada, and the AS in Australia. Our experiments have relied on the use of Beamlines 1.4.3, and to some extent 1.4.4 at the Advanced Light Source in Berkeley CA.

Our primary interest in developing SIRM for rhizosphere studies has been to use the mid-IR spectroscopic signatures of organic and inorganic compounds as noninvasive contrast reagents for microscopic examination (and mapping) of the root zone. Whenever scientists have been provided new imaging technologies (microscopic or telescopic), new, scientific vistas have opened. By coupling synchrotron radiation (SR) sources with mature IR microscope technology (Reffner et al., 1995), we can image the rhizosphere of intact plants to observe that plants

- actively mine the environment for nutrients,
- make heavy metals less toxic to themselves,
- defend themselves from predators, and
- establish useful symbioses and associations with soil microbes.

The term "rhizosphere" was first coined by Hiltner (1904) to describe the region of intense biological and chemical reactivity near the surface of growing plant roots. A mixture of plant-initiated and microbially expedited transformations turns the region (within a few millimeters of the roots) into a complex best described through the principles of community ecology. Plant roots may, with chemical exudates, attract new microbial associations (Peters and Long, 1988; Yoder, 2001), improve water-retention in the root zone (Clifford et al., 2002), solubilize soil nutrients (Dinkelaker et al., 1989; Fan et al., 1997), immobilize phytotoxic metals (Kochian, 1995; Watanabe et al., 2008), defend themselves from root-predators (Makjanic et al., 1988), or inhibit root growth of competing plants (Bertin et al., 2007; Mahall and Callaway, 1991). In light of this multichannel, multipurpose communication, techniques for the identification and characterization of root exudates are essential. If it were possible to "see" through a

Author's personal copy

reasonable thickness of the soil fabric, then we could estimate rates of diffusion in the soil for root exudates, and conceivably back-calculate their production and/or consumption rates (Schmidt and Ley, 1999; Schmidt et al., 2000). This has been the vision for the "rhizobox" work.

Some biological justification for our "model" plant systems is in order. We initially chose to analyze root exudate responses within the: (1) Leguminosae, (2) Brassicaceae, and (3) ferns. The legumes are a large plant family containing both wild and cultivated relatives, including such familiar species as common beans, lentils, clovers, lupins, etc. (Sumner, 2000). From both the economic botany as well as ecosystem perspective, legumes reign supreme among plant families in the world because of their capability of fixing atmospheric N_2(g) to organic N. The actual fixation of nitrogen in these plants represents a collaborative effort with naturally occurring soil bacteria, principally species of the *Rhizobia* or *Bradyrhizobia* that form symbioses on the roots of legumes, or the nitrogen fixing actinomycete *Frankia*, capable of root-associations with members of at least eight families of angiosperms (Myrold, 1994). So, it was reasonable to work-up synthetically from nonnodulated seedlings → fully nodulated → mycrorrhizal, nodulated plants and ask, at every step: "Does the essential nature of the exudates change over the formation of the tripartite symbiosis ?"

Because of their unique symbioses, nitrogen-fixing plants are a major source of edible protein worldwide, and under intense scrutiny in the developing nations of South America and South Asia for restoration of degraded pasturelands and upland soils (Rao et al., 1993). Erodible soils in the neotropics can suffer irreversible losses of fertility if left uncovered after cattle ranching or other extractive industries. Therefore, any planting system contributing carbon to the soil is a plus in terms of mitigation of greenhouse gases (long-term), or soil erosion (short-term and long-term). To evaluate germplasm for such restoration projects, identifying and comparing differences among the compounds exuded by roots will inform the eventual success of such projects. Beyond the basic questions considered in the previous section, we believe that SIRM contributes directly to CO_2-abatement research, since most of the Consultative Group on International Agricultural Research (CGIAR, or "Green Revolution") laboratories opted for a "molecular breeding" approach to the exploration of variability in wild germplasm (Rao et al., 1993, 1999). When breeder-physiologists or ecologists rank the "performance" of plants, it is almost always with respect to leaf-associated characters. Can we meaningfully develop nondestructive screening tools (with the long-term goal of rehabilitating lands) that evaluate root properties ?

To give a concrete example, consider the condition of low-base status in a widespread class of tropical soils. The low fertility and base cation status of Ultisols has been, and in many areas continues to be, the major limitation to their agricultural use (Buol et al., 1973; Sanchez, 2002). These soils possess low pH and high levels of free Al^{3+} in their surface horizons from natural mineral weathering/dissolution (Sposito, 1989). Aluminum in uncomplexed form is toxic to plant cells (and many other organisms), and researchers have discovered that plants tolerate toxic Al^{3+} levels by excreting large amounts of malic acid (Kochian, 1995; Ryan et al., 1995) into the space surrounding the roots so as to reduce the free activity of Al^{3+}. Several questions pose that may be tested with the rhizobox/IR microscope methodology described in this chapter:

- How common is this malate-response among legumes ?
- Are there differences among wild and cultivated legumes ?
- Are additional compounds exuded that may be involved as well ?

From a fertility point of view, some tropical soils evince two main constraints that we seek

Author's personal copy

to address in our visualization studies with synchrotron IR—low phosphorus status and aluminum toxicity. Can plants be selected to respond well to both stressors? Support for the view that commonalities exist in the response of plants to low P/high Al arises from recent plant genomics research demonstrating considerable overlap in the identity of genes activated in short-term root responses (Chandran et al., 2008; Hirai et al., 2004; Kochian et al., 2004; Muller et al., 2004), though additionally, several plant families have evolved architectural strategies to compensate for the low intrinsic mobility of phosphate in soils (Kochian et al., 2004; Roelofs et al., 2001).

Our purpose here is to demonstrate that SIRM images and spectrally identifies particularly abundant polar compounds in the root zone, based on the presumption that such compounds influence overall soil chemistry and weathering processes (Banfield et al., 1999). It is worth mentioning that thermal IR spectra demonstrate certain biases among the compounds on which they report—strong IR signals arise from chemical bonds of strong polarity, and perhaps it is no accident that some of the most common biochemical moieties that bind metals in nature with high affinity include acidic carboxylic functionalities ($-COO^-$), esters (>C=O), and hydroxyl (–OH) groups, and that they are quite distinguished by IR spectroscopy. Strong electronegativity differences in the constituent atoms of functional groups ensure high IR signal intensity; likewise, large reduced masses ($m_1m_2/(m_1 + m_2)$) for two bonded atoms (of masses m_1 and m_2) ensure that the bands will occur at high IR energies. The last "bias" actually presents an opportunity for combining rhizobox studies with better-known isotopic-labeling methods, as portions of the thermal IR are devoid of absorbance features; judicious application of, for example, $^{13}CO_2$ can shift the fundamental frequency of a labeled band into a region that clarifies the source of the absorbance due to lack of clutter. One of the first applications made accessible by rhizosphere-imaging methods resides in the comparative root-exudation profiles of a confamilial group of cultivated plants exposed to phosphorus nutritional deprivation. In many previous studies researchers identified simple carboxylic acids of the Krebs' cycle (Dinkelaker et al., 1989; Lipton et al., 1987), phenolic acids (Ae et al., 1990), and pH-changes in the root zone (Blanchar and Lipton, 1986; Marschner et al., 1982) as P-availability increased. Over the last few years, as whole-genome studies of model systems such as *Arabidopsis* and rice became available, identification of the transcriptional network of genes responding to P-deprivation have mushroomed (Hirai et al., 2004; Muller et al., 2004). We feel confident that the combination of direct observation of rhizosphere exudates by SIRM in combination with transcriptional studies will uncover novel tolerance mechanisms, beyond those described in physiological and biochemical studies, and expand the knowledge base of plant transporters involved in shuttling C to the rhizosphere.

The mustard family was chosen principally for two reasons; it is one of the very few plant families worldwide found in a nonmycorrhizal state, and the family has a well-earned reputation of rich, sulfur-based secondary chemistry; easily polarizable d-level electron orbitals in C-S bonds provide mustards with a fearsome affinity for transition metals. Broccoli Raab (*Brassica rapa* L. var. cymosa) is phylogenetically close to the black mustards receiving much attention in the bioremediation literature (Bañuelos et al., 2004). We began the rhizosphere studies a year (1999) before the publication of the *Arabidopsis* genome sequence (the first plant to have its entire genome sequenced), and while spectroscopy and genomics may seem a logical combination, the size and growth habit of *Arabidopsis* are not typical of the Brassicaceae on the whole, and we have thus confined our synchrotron studies in this

Author's personal copy

organism to leaf traits, esp. cell wall biochemistry and powdery mildew susceptibility (Raab and Vogel, 2004; Vogel et al., 2004).

Though ferns have only recently begun to be appreciated by molecular biologists as model systems in cell biology (Strain et al., 2001), ecologists have long appreciated their abundance (and occasional dominance) in temperate and tropical ecosystems. Throughout the humid tropics, landslides are often quickly colonized by ferns, including the mat-forming ferns of the genus *Dicranopteris* (Walker and Boneta, 1995). Modern molecular phylogenetic work on ferns (Smith et al. 2006) highlights a dichotomy in the apparent evolutionary history of two major lineages—the modern "polypod" ferns, and an older lineage of "Core Leptosporangiate" ferns which radiated tens of millions of years prior to the diversification of angiosperms. A deeper understanding of their root systems and chemical effects on young landscapes may thus be of interest to paleobiologists and soil scientists. A related area, and one which has received little attention by ecophysiologists, is the issue of fern mycotrophy. During their life cycle, ferns may display fungal infection in their thalli, rhizomes, or roots (Powell and Bagyaraj, 1984), and microscope surveys (Read et al., 2000) support the existence of some AM-associations in basal fern lineages such as the Gleicheniales. As we allude to in the introductory section of this chapter, it is reasonable to ask whether the presence/absence of mycorrhizae leads to a "ripple-effect" on subsequent microbial colonization. The first fern selected (on the basis of compact genome size and the speed with which it transitions from gametophyte to sporophyte) for genome sequencing was *Ceratopteris richardii*, a subtropical fern of semiaquatic growth habit, and member of a modern fern family. Easy to culture in the lab, it was one of our first experimental species for rhizobox experiments, as it comes from a nonmycorrhizal fern lineage. In some ways, *Ceratopteris* represents a marginal "model plant" for tropical biogeochemistry insofar as the bulk of extant ferns have a terrestrial habit; on the other hand, only a small number of ferns can be quickly and reproducibly cultured to their sporophytic form.

6. CHARACTERIZING AND IMPROVING RHIZOBOX TECHNOLOGY: IR OPTICS ISSUES

Plant biologists have long sought a method for the repeated analysis of root properties and growth without recourse to excavation and disturbance of the soil (Steeves and Sussex, 1989). We grow seedlings for SIRM in "rhizoboxes," not unlike the early designs of Polonenko and Mayfield (1979) and Faber et al. (1991). The Lexan faces of the rhizobox have been modified with zinc selenide (ZnSe) windows (Raab and Vogel, 2004) to allow IR transmission (Fig. 7.2). Root boxes (dimensions 25 × 10 × 1.25 cm) were constructed of polycarbonate in two pieces, one solid backed with a drain slot, and a second thinner piece for the front of the root box having a machined slot for the ZnSe, IR-transmissive window. The window is a trapezoid (Janos Optical; VT) of dimensions 50 × 20 × 1 mm. ZnSe is a chemically neutral, translucent, polycrystalline material with no significant visible/IR absorption over the wavelength range 0.5-18 μm. On the downside, the high refractive index of the material (n = 2.4) leads to reflection losses of ~17% per surface. Materials appropriate for IR microscopy are limited—while salt windows (e.g. NaCl, KBr) have broad IR transmission, they fog easily and eventually dissolve in the moist environment of roots. While many metallic semiconductors like germanium (Ge) also transmit over a wide range in the mid-IR and parts of the visible region, visual microscopic examination is difficult. Wetzel (2002) has advocated for diamond windows, in part due to their lower index of refraction and ease of

Author's personal copy

FIGURE 7.2 Rhizobox with tobacco seedling growing in silt/sand mixture, 18 days after sowing, showing inset ZnSe window. Boxes can be covered with Al-foil to suppress algal growth.

focusing for spectromicroscopy; however, price is still an obstacle for the use of custom-made CVD-diamond windows. As a compromise, ZnSe is a polycrystalline material with broad transmission in the visible and mid-IR (low energy cut-off at 454 cm^{-1}), and most importantly, is chemically neutral, reacting imperceptibly with soil water or roots during the course of experiments. The window is held in place on each rhizobox with two Teflon washer-screw combinations; metal should be avoided due to strange electrochemical deposition on the windows. Prior to mounting, the window is carefully wrapped in Al-foil with a small 0.5 mm-diameter hole cut into the foil. The foil-window assembly is then placed in a vacuum deposition apparatus at a scanning electron microscope facility, and gold is deposited at low current for 50 s over the hole in the Al-foil mask. The gold is deposited on the root-zone facing side of the window, and serves as an internal reflection standard for the IR beam. Thus, the ratio of single-beam spectra acquired in reflection mode from soil or roots to this internal Au reflection standard can be found and more familiar absorbance or reflectance spectra can be calculated.

7. PLANT-CULTURE ISSUES

The two portions of the rhizobox were secured with large clips, wrapped on two sides with aluminum foil to limit algal growth, and held upright at a slant in the greenhouse. Each root box was fitted with a 40-mesh nylon drain screen at the bottom to permit free gravity-drainage of water and improved aeration. Horticultural sand was acid-washed (1 M HCl) and vigorously rinsed with distilled water after soil sieving to $\geq$53 μm particle size. After air-drying, the sand was loosely packed into the upright root boxes, taking care not to unnecessarily scratch the ZnSe observation windows. Seeds of various legume species were lightly pressed into the sand to a depth of 3 mm, and the microcosms watered and fertilized for optimal growth of legumes (Fredeen et al., 1989), including the addition of both Co^{2+} and Ni^{2+} at 10 μM final concentration. Plants were fertilized once every other week, and watered as needed with 18 MΩ.cm distilled water, until excess drained from each rhizobox. The root boxes received natural sunlight in a temperature-controlled greenhouse. Roots growing near these windows allow direct spectromicroscopic observation of the root-soil interface zone. The ultrahigh brightness of the SR beam allows us to focus the IR down to a spot-size with an average size of 6-10 μm (Levenson et al., 2008; Martin and McKinney, 1998) without losing

Author's personal copy

the intensity of the signal (Martin et al. 2001). This is simply not possible with a conventional thermal "glow-bar" source and IR microscope (see Reffner et al., 1995), where spot-sizes might be 30-40 μm in each dimension. The small spot size of beamline 1.4.3, in conjunction with the computer-controlled *x-y* positioning stage of the IR microscope, allows mapping of the spatial distribution of organic (and mineral) compounds found in the rhizosphere of plants.

Seeds germinate directly in the rhizoboxes, and after some time, roots grow past the ZnSe observation windows. This provides a snapshot of the root-soil-water interface zone for an intact plant. We can now subject the plant to nutritional stress, heavy-metal toxicity, pathogen attack, or climatic stress and observe the temporal progression of root exudate response(s)—and most importantly, *repeat the measurements some days or weeks later*. Currently, rhizobox geometries are limited to small herbaceous plants and ferns, but it may be possible to extend the methods to small tree seedlings in the future. Mung beans grown in the rhizoboxes expressed large, branching root systems, some coinciding with the ZnSe observation window (tested up to 8 weeks after germination). Within 72 h following germination of the mung beans in the IR rhizoboxes, we detected strong polysaccharide modes from large "ribbons" of material that seemed to be expelled from the seed case. A strong trio of absorptions at 1181 cm^{-1}, a shoulder at 1145 cm^{-1}, 1086 cm^{-1}, and a weaker feature at 1043 cm^{-1} were observed. At higher energies, absorptions at 1682, 1557, 1393 cm^{-1} arose from the complex modes of proteins (i.e., amide-I and amide-II), and small admixtures of pectic polysaccharides (Fig. 7.3A). Initial IR spectral database searches using a correlation algorithm (available on the OMNIC 6.2 software; Thermo-Nicolet, Madison WI) for the region 900-1300 cm^{-1} showed a strong match for mannan-containing polysaccharides. The tentative assignments of these absorptions are to the ribbon-like seed polysaccharides galactomannans. These compounds are neutral α-(1,6) branched polymers of galactose on a β-(1,4) mannose backbone. The spectra has an additional small, but unmistakable absorbance at 994-998 cm^{-1} in the so-called "anomeric" region of the mid-IR where sugar chains may be distinguished based on the stereochemistry of their principal linkages (Kacurakova et al., 1990; Mathlouthi and Koenig, 1986). It has also been possible to simultaneously extract these polymers from mung bean seed coats using standard gas chromatography methods (Raab et al., 2010), and confirm that a gal-man polymer is the principal sugar-bearing component of the visual image. Legume seeds (esp., soybean, alfalfa, and carob) as well as green coffee beans are rich in galactomannans, and ~75% of common feed legumes contain such "mucilage yielding" endosperms. The mannans are able to form very hard, crystalline structures, and are remarkable for their structural similarities to cellulose. Per unit dry weight, galactomannans are about fivefold higher in viscosity than starch, making them some of the most viscous polysaccharides known.

In all cases, the mung beans expressed large branching root systems, some portion of which was coincident with the ZnSe observation windows. In Figs. 7.3-7.5, you see "screen-grabbed" images through the 15× objective of the SIR microscope of an intact, nodulated *Vigna mungo* seedling, mucilage network of the edible mustard *Brassica rapa* var. rapus (broccoli Raab), and a wild legume *Lupinus sparsiflorus* L. growing in IR-rhizoboxes. IR reflectance spectra obtained of the root zone through the IR microscope demonstrated significant differences in mung beans exposed to low-P conditions as compared to the nutrient-sufficient plants (Fig. 7.3C; Raab and Martin, 2001). The region below 2000 cm^{-1} in the mid-IR is known as the "fingerprint region," and particularly noticeable were strong IR absorption features between 1150 and 850 cm^{-1} in

Author's personal copy

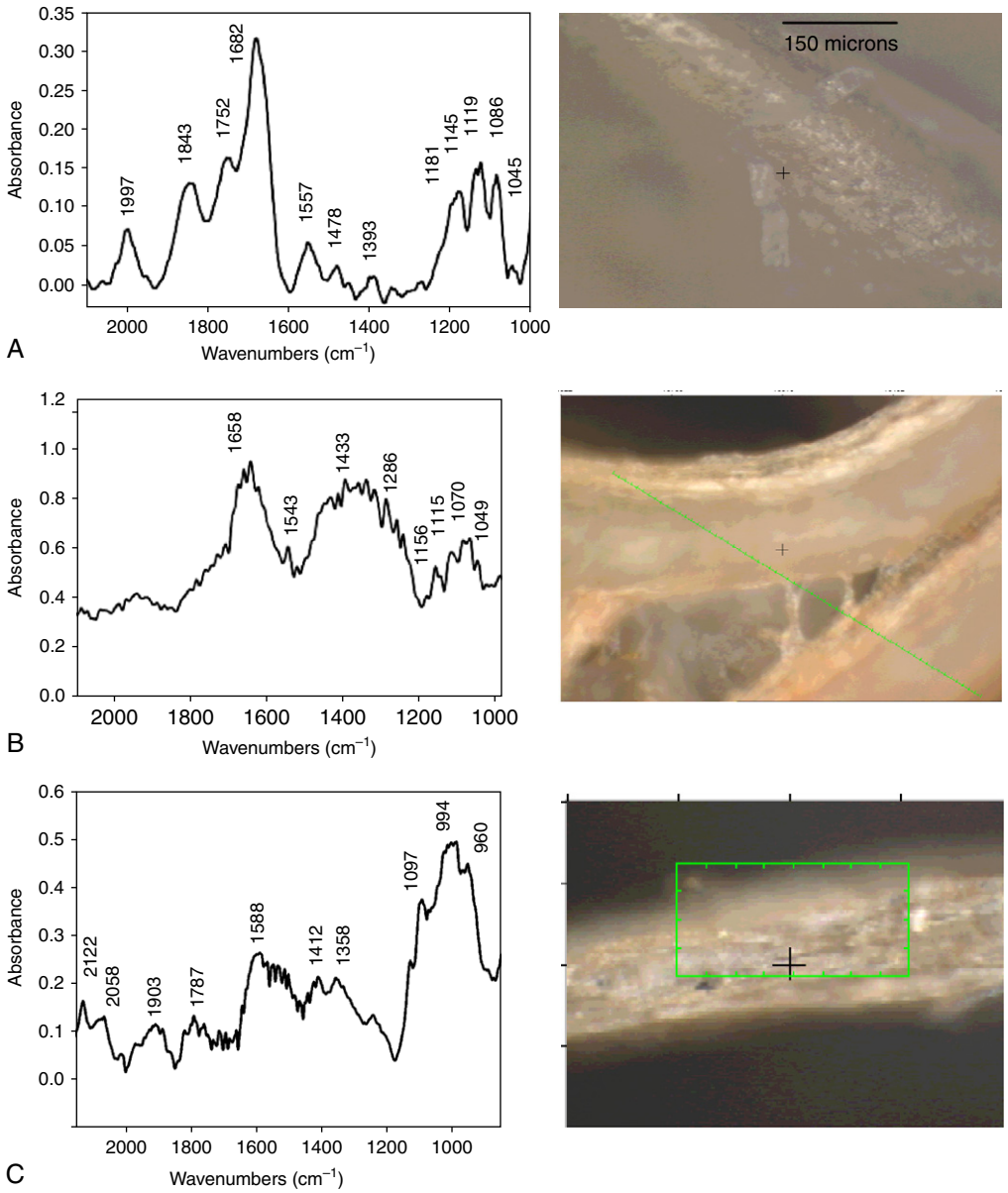

FIGURE 7.3 Linked thermal IR reflectance spectrum and low magnification image (15× IR objective) of: (A) cultivated mung bean (*Vigna mungo)* seed mucilage ribbons, 3 days after germination [*Band assignments*: 1997 cm^{-1} (asym N=C=S stretch), 1843 cm^{-1} (>C=O asym stretching), 1752 cm^{-1} (ester carbonyl stretch), 1662 cm^{-1} (protein amide-I), 1557 cm^{-1} (protein amide-II), 1478 cm^{-1} (ester > CH_2 sym deformation), 1393 cm^{-1} (aldehyde C–H deform), 1181 cm^{-1} (mannan C–O–C ring mode), 1145 cm^{-1} (mannan C–OH), 1119 cm^{-1} (pectin [νCCνCO]), 1086 cm^{-1} (mannan), 1045 cm^{-1} (pectin).] (B) nodulated root junction of *Vigna* [*Band assignments*: 1658 cm^{-1} (protein amide-I), 1543 cm^{-1} (protein amide-II), 1433 cm^{-1} (ether C–H sym. deform), 1286 cm^{-1} (aromatic amine C–N stretch), 1156 cm^{-1} (C–O stretch), 1115 cm^{-1} (aromatic sym. C–O–C stretch), 1070 cm^{-1} (alicyclic ring C–O stretch), 1049 cm^{-1} (arabinogalactan ring mode)]. Scale bar = 150 μm. (C) nonnodulated *Vigna* root [*Band assignments*: 2122, 2058 cm^{-1} (possible isothiocyanate doublet), 1903 cm^{-1} (2 ° amine ?), 1787 cm^{-1} (C=O stretching vibration), 1588 cm^{-1} (Amide II, N–H deformation and C–N stretching vibration), 1412 cm^{-1} (lipid C–H asym. deformation), 1358 cm^{-1} (polysaccharide C–H and O–H deformation vibration), 1098 cm^{-1} (siloxane Si–O stretch), 994 cm^{-1} (asymmetrically P–O–C stretching vibration ?), 960 cm^{-1} (starch α-anomeric band)].

Author's personal copy

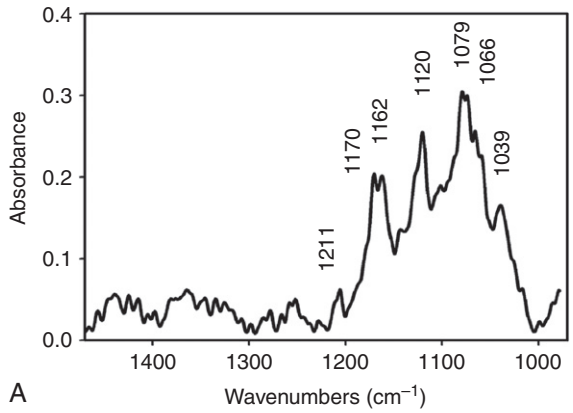

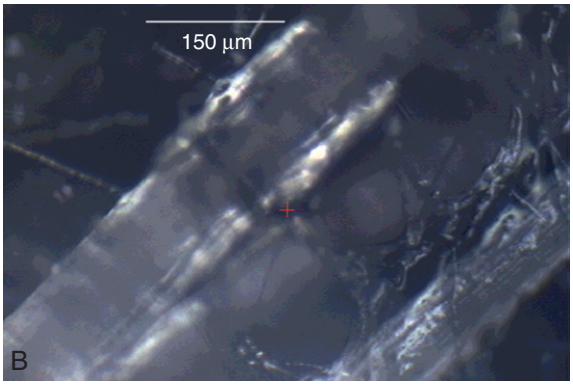

FIGURE 7.4 Linked mid-IR spectrum and low magnification IR-microscope image of the cultivated mustard *Brassica rapa* roots and associated mucilage network, 28 days after sowing [*Band assignments*: 1211 cm^{-1} (phenolic C–O stretch?), 1170 cm^{-1} (cyclic ether C–O stretch), 1162 cm^{-1} (cellulose), 1120 cm^{-1} (cellulose C–OH), 1079 cm^{-1} (xyloglucan C–O–C), 1066 cm^{-1} (arabinogalactan C–O–C), 1039 cm^{-1} (arabinan ring-mode)].

the low-P treated mung beans. For mapping points acquired directly on the root surface of nutrient-sufficient mung bean, we observed (Raab and Martin, 2001) strong absorbance features at 1627, 1399, and 1269 cm^{-1}, and weaker ones at 1003 and 775 cm^{-1}. In contrast, the root surface of nutrient-sufficient mung beans demonstrated dominant IR absorption features from cellulose at ~1000 cm^{-1}, with small, sharp bands at 1090 cm^{-1} and an unresolved mass at 750 cm^{-1}. The very small spot size at BL 1.4.3 of the ALS, in conjunction with the computer-controlled *x-y* positioning stage of the IR microscope, allows us to map the spatial distribution of a variety of organic compounds found in the rhizosphere of plants. "Hyperspectral" maps may be either collected along a line (as seen in Fig. 7.3B), or over a 2D grid. It will be appreciated that line scans are particularly useful for mapping gradients of soluble compounds in the root zone of intact plants. While not necessary and sufficient evidence in itself that exudation is in fact occurring, these IR scans serve a useful heuristic role in focusing more elaborate chemical methods (Fan et al., 1997; Fiehn et al., 2000; Kuzyakov et al., 2003) toward the identification of root signals. In the figure legends for the IR spectra, we provide the best matches for spectral bands with strong S/N ratios; *band assignments* are based on pure compound studies performed in the author's lab, as well as Farmer (1974), Mathlouthi and Konig (1986), Coimbra et al. (1998), Jamin et al. (1998), Kacurakova et al. (2000), Synytsya et al. (2003), and Yu (2007).

What were our major observations from manipulating phosphorus levels in legume rhizobox experiments? (1) It is possible to grow both cultivated and wild legumes in thin sand/silt-culture rhizoboxes from seed to seed, with or without nodulation for IR spectromicroscopy; (2) when deprived of phosphorus, *Vigna* bean root growth increases at the expense of shoot growth, (3) roots of low-P *Vigna* have lower specific root length, and correspondingly lower levels of lignification compared to control plants as determined by IR microscopy, (4) IR spectra from low-P rhizospheres show a wider variety of organic acids, sugars and protein components than the root zone of control plants, and (5) root exudates of cultivated and wild legumes differed in chemical composition. In rhizobox experiments with legumes, both cultivated (*Vigna*) and wild (*Lupinus*), we observed IR absorbances suggesting allene- and isothiocyanate-based

Author's personal copy

antiherbivory compounds or precursors, previously known from legume seeds. IR reflectance spectra collected by the synchrotron IR microscope demonstrated significant differences in nodulated mung beans as compared with nonnodulated seedlings (Fig. 7.3B,C). First and foremost, there are higher concentrations of protein in the nodulated mungbean rootzone, and a distinct set of polysaccharides contributing to the exudate complex. Given uncertainties over IR band extinction coefficients for polymers (and the degree of metal binding to the exudates), we suggest that protein exudation (per unit polysaccharide) in nodulated legumes appears to be 50-75% higher than observed in nonnodulated cases.

In most cases, microscopic examination of intact, growing plants yield spectra comparable to those that may be collected from either thin-sections of plant tissues (Wetzel and Reffner, 1993; Yu et al., 2003), or purified biochemical preparations (Zeier and Schreiber, 1999) of root components. Again, there are not many alternative methods that currently provide such detailed chemical information on intact plant tissues in a nondestructive fashion at these spatial scales, other than perhaps Raman microspectroscopy, a complementary technique to SIRM (Gierlinger and Schwanninger, 2007), and possibly secondary ion mass spectrometry (SIMS), which provides stable isotope ratios at very fine spatial scales. Unfortunately, Raman methods suffer from unavoidably high fluorescence backgrounds for many plant materials (esp. lignin-rich tissues), although development of new sampling strategies continues.

For experiments with *Brassica rapa* we inquired whether nonmycorrhizal plant species have fundamentally different exudate profiles from other plants. In our preliminary characterizations, they did differ from legumes (both wild and cultivated) in the sense of being enriched in polysaccharides, possibly at the expense of N-containing compounds. Common to all hydrated samples are broad –OH features centered at 3500 cm^{-1} and water vapor features (that can be subtracted from spectra) from 4000-3500 cm^{-1} to 2000-1400 cm^{-1}. Common as well to all spectra collected from actively respiring root systems is the strong IR "Fermi doublet" of CO_2 at 2360 cm^{-1}. Useful markers for root tissue are the multiplets from 2950-2850 cm^{-1}, arising from stretching modes of methyl/methylene groups in cuticular lipids. Ratios of IR absorbance in this region can be used to derive average chain-lengths of surface waxes (Merk et al., 1998). Additional lipid-related compound matches obtained from imaging *Brassica* seedlings were 12-hydroxydodecanoic acid, and 1,8-octanedioic acid (also known as "suberic acid." Among the species we surveyed, suberized cell sloughing into the rhizoboxes was by far most prevalent in *Brassica rapa*.

8. POLYURONIC ACIDS IN ROOT MUCILAGE

Pectin influences a range of plant cell properties by virtue of long stretches of acidic unesterified galacturonic acid residues which associate through Ca^{2+}- mediated cross-bridges (Jarvis, 1984; Morris et al., 1982; Willats et al., 2001). Binding of Ca to the cell wall largely scales with the density of the negative charge carried by the cell wall, itself governed by the degree of methylation of pectin. The high charge-to-ionic size ratio of Ca^{2+} ions leads to rapid and strong binding to pectin with a low degree of methylation. These associations lead to a gel with ion exchange properties and variable pore size, allowing proteins (including foreign hydrolases) and polysaccharides <50 kDa molecular weight to diffuse across the wall within an hour.

The unique ion-exchange behavior of pectins does not merely confine its influence to plants' internal cell wall architecture at small spatial scales, but in fact also contributes a source of acidity to the soil fabric capable of weathering

Author's personal copy

soil minerals in upper horizons. A case in point is root mucilage, carbohydrate polymers characterized by high charge densities associated with free carboxyl groups on constituent uronic acid sugars—principally galacturonic acid/glucuronic acid in higher plants, and guluronic and mannuronic acids of algal EPS. Extracellular polysaccharides from algae and certain bacteria are acknowledged to participate in mineral weathering reactions (Welch et al., 1999). This study indicated that acidic pectin or alginate polymers exogenously applied to soils were 3-30 times more effective in de-silification of minerals than "neutral" polymers such as starch. Pectin polymers derived from plants are likewise abundant and observed at the soil-root interface and are the major high molecular weight compounds exuded by roots (Figs. 7.3, 7.4B, and 7.5B; Raab and Vogel, 2004). This hydrophilic "mucilage," mainly composed of short fibrils of calcium-polyuronic acids, scaffolds the cation exchange capacity (CEC) of root cell walls. Methylesterification of this pectin network determines the CEC of the root's apoplastic space (Dufey and Braun, 1986); increased methylation of uronic acids in the root cell wall decreases root CEC, and consequently, decreased root CEC reduces binding of Al and Ca to the cell wall. These properties explain the apoplast's ability to form complexes with heavy metal analogues of calcium (e.g., Pb^{2+}, Cd^{2+}), as well as micronutrients such as Cu^{2+} (Kono et al., 2005). This results in diffusive exchange of metal cations on pectins due to their acidic properties.

Ceratopteris richardii, a subtropical fern of semiaquatic growth habit, is easy to culture in the lab, and was one of our first experimental species for rhizobox experiments, as it comes from a modern, nonmycorrhizal fern lineage. Modifying the widely available nutrient media for *Ceratopteris* (Hickok et al., 1995) to provide nutrient-sufficient and low-phosphorus conditions, we compared the rhizoid structure and rhizosphere chemistry of *Ceratopteris* plants

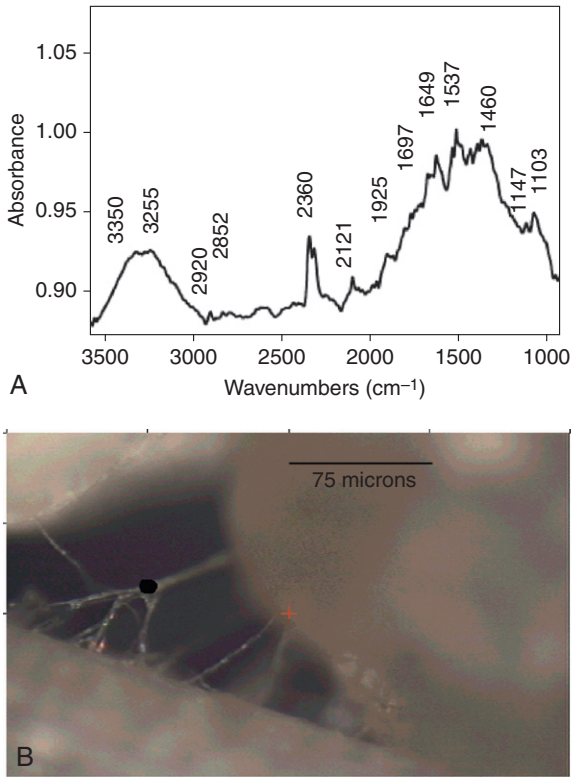

FIGURE 7.5 Linked thermal IR spectrum and low magnification image of wild legume *Lupinus sparsiflorus* roots and associated mucilage network forming multiple strands anchoring sand and silt particles in a rhizobox (28 days after sowing) [*Band assignments*: 3350 cm^{-1} (carbohydrate –OH, w/internal H-bonding), 3255 cm^{-1} (protein –NH), 2920 cm^{-1} (>CH_2 asymm stretch), 2852 cm^{-1} (methylene, C–H sym stretch), 2360 cm^{-1} (CO_2 Fermi doublet), 2121 cm^{-1} (N=C=S stretch, isothiocyanates ?), 1925 cm^{-1} (allene asymm C=C=C stretch), 1697 cm^{-1} (α,β-unsat'd. amine C=C stretch), 1649 cm^{-1} (protein amide-I), 1537 cm^{-1} (protein amide-II), 1460 cm^{-1} (lipid ether linkage C–H asym deform.), 1147 cm^{-1} (glucoronoxylan C–OH), 1103 cm^{-1} (divalent salt pectate CO/CC/CCH/OCH ring mode)].

using IR methods. In some ways, *Ceratopteris* represents a marginal "model plant" for tropical biogeochemistry insofar as the bulk of extant ferns have a terrestrial habit; on the other hand, only a small number of ferns can be quickly and reproducibly cultured to their

Author's personal copy

sporophytic form. Figure 7.6 compares the "fingerprint region" of average exudates from *Ceratopteris* plants supplied full nutrients, or deprived of phosphorus. Both exudate profiles have comparable intensities for protein and polysaccharides, though low-P ferns had a larger contribution from hemicellulosic sugars (1163 and 1127 cm^{-1}) and cuticular fragments (the latter judged by $>CH_2$ ν_a at 2935 cm^{-1}, wagging modes at 1344 cm^{-1}, and δ-scissoring at 1461 cm^{-1}), and a conceivably lower contribution of nucleic acids. One model to explain this is that the low-P *Ceratopteris* plants were turning over fine root cells at a faster rate than nutrient-replete plants. Based on a comparison of the two treatments' sugar ring modes between 1170-980 cm^{-1}, nutrient limitation fundamentally reorients root C-reserves to exudation. One puzzling observation in this regard is the more pronounced methyl- (or *o*-acetyl-) esterification associated with exudates from the low-P ferns (i.e., the height of the shoulder at 1742 cm^{-1}). This spectral assignment requires additional biochemical tests, since the ester groups might arise from fragments of suberin lipids and/or lignin derivatives. Considering the high energy region from 3700-3000 cm^{-1} (spectral region not shown in Fig. 7.6), the lignin idea seems less likely, insofar as the control *Ceratopteris* had an absorbance at 3062 cm^{-1} (aromatic –CH stretch) absent from low-P. Overall, the chemical modulation of root exudates by parent plant nutrient status is not entirely surprising, yet no robust theory accounts for it.

Synchrotron-based hard X-ray tomography (a technique not covered in this chapter explicitly) led Feeney et al. (2006) to provide an interesting perspective on some of our IR microscopy studies of the rhizosphere. By comparing soil microcosms with and without the grass *Lolium perenne*, the authors compared the "coherence length" of soil structure and porosity, and found that the region near the roots (rhizosphere) had higher porosity as well as significantly longer "coherence lengths" than

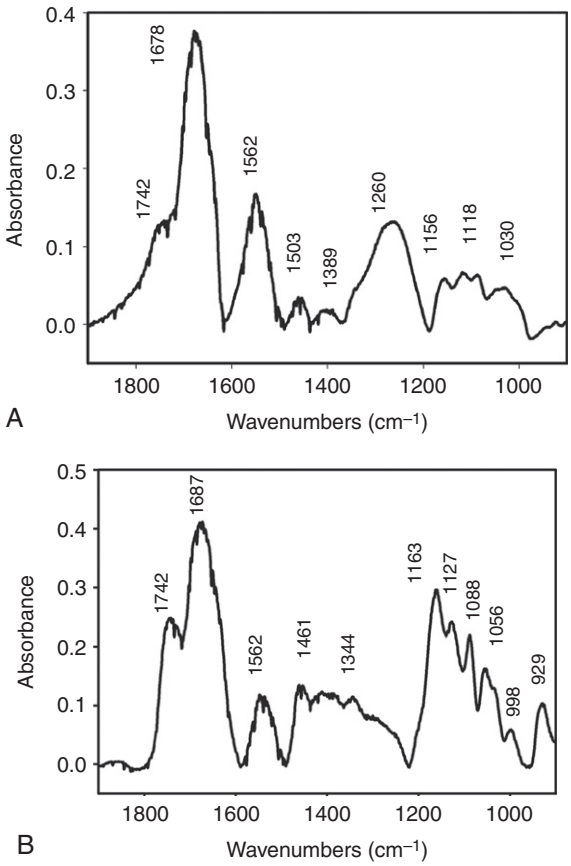

FIGURE 7.6 IR reflectance spectra from rhizoid exudates of the semi-aquatic fern *Ceratopteris richardii*. Top spectrum (A) is from nutrient-replete ferns, and the lower spectrum (B) from low-phosphorus plants [*Band assignments*: (A) 1742 cm^{-1} (ester C=O stretch), 1678 cm^{-1} (protein amide-I), 1562 cm^{-1} (protein amide-II), 1503 cm^{-1}, 1389 cm^{-1} (phenolic combination. O–H deform and C–O stretch), 1260 cm^{-1} (phenolic δ- $(OH)_{alc}$ deform), 1156 cm^{-1} (C–O stretch), 1118 cm^{-1} (asym. C–O stretching vibration ?), and 1030 cm^{-1} (pectin or glycan C–C ring mode); (B) 1742 cm^{-1} (ester C=O stretch), 1687 cm^{-1} (protein amide-I), 1562 cm^{-1} (protein amide-II), 1461 cm^{-1} (lipid δ-scissoring), 1344 cm^{-1} (lipid $>CH_2$ wagging), 1163 cm^{-1} (cellulose C–OH stretch), 1127 cm^{-1} (CO, CC stretching), 1088 cm^{-1} (2° alcohol C–O stretch), 1056 cm^{-1}, 998 cm^{-1} (polyuronic acid ring mode), 929 cm^{-1} (β-anomeric band, cellulose acid)].

Author's personal copy

bulk soil, on the order of 320 μm. The root mucilage seen in Figs. 7.3B, 7.4B, and 7.5B represents filaments of nearly this length. The biological effect on soil orientation has been variously interpreted as providing anchorage for establishing seedlings, for orienting soil particles (Yaci et al., 2005), and increasing the tilth of soils.

9. SCANNING TRANSMISSION X-RAY MICROSCOPY APPLICATIONS IN ECOLOGY

Our most recent application of SR was in the soft X-ray regime (see Fig. 7.1), using STXM for direct tests of the stoichiometric theory of ecology, pinpointing, in a sense, the "trophic level" of bacteria or fungi in the rhizosphere. Recent work by Loreau and coworkers (Daufresne and Loreau, 2001) leads to a reconsideration of which trophic levels within the soil determine limiting nutrient levels for plant growth. Do herbivores always set the tone? To what extent do decomposers dictate nutrient limitations in terrestrial ecosystems? Nutrient cycling within ecosystems can be viewed as a consequence of groups of organisms with very different energy sources (autotroph vs heterotroph, consumer vs decomposer) and characteristic biochemistries and stoichiometries making their livings in the same place—with the tissues and/or waste products of each group being the fundamental resources for some or all of the others. If we compare bacteria and fungi, differences in growth form (single-cell vs multicellular hyphae) and degradative physiology are important attributes differentiating the competitive abilities of these organisms. In particular, fungi produce oxidative enzymes with the capability to decompose lignin polymers—whereas bacteria are faster growing and possess a competitive advantage for soluble smaller carbon compounds. Through hyphal extension, filamentous fungi have the ability to penetrate voids in plant cell walls, thereby gaining internal access to cellulose which most soil bacteria cannot. Most soil bacteria and actinomycetes cannot completely depolymerize cell wall lignin. In contrast to bacteria, filamentous soil fungi can move nutrients to the site of degradation via hyphae extending from decomposing litter into soil (Wallander and Pallon, 2005). As well, bacteria and fungi may have varying nutrient requirements—in particular, bacteria require more N, whereas fungi may require more Ca.

For chemical elements, the long-standing focus on carbon, nitrogen, and phosphorus is understandable given their fundamental roles in biological structure and metabolism, and because N and P supply often limits the growth of organisms and the rate of ecosystem processes (Vitousek and Howarth, 1991). However, nearly 20 additional elements are essential to the growth of plants, animals, or both—and some of these can control particular organisms and processes in many ecosystems, and overall ecosystem functioning in some. Of these additional elements, Ca is perhaps the most interesting. The distribution of many plants, plant communities, and ecosystem properties is highly correlated with soil Ca^{2+} (McLaughlin and Wimmer, 1999). Despite covariance between Ca^{2+} and soil pH (and other factors), there is good evidence that Ca^{2+} supply itself constrains biological processes in two widespread circumstances: (1) Where soils are coarse-textured, and the parent material resistant to weathering, Ca^{2+} and other cations can be leached rapidly enough to deplete available Ca^{2+}—particularly where anthropogenic acidity enhances cation mobility (Likens et al., 1998). Ca^{2+} supply may then limit rates of biological processes, though enhanced rates of weathering may counteract Ca^{2+} depletion (Blum et al., 2002). (2) Where old soils in the humid tropics and subtropics have been depleted by tens of thousands to millions of years of weathering and leaching (and as discussed in the legume rhizobox experiments),

Author's personal copy

their ability to supply cations can be lost irretrievably (Chadwick et al., 1999). Consequently, many tropical forest ecosystems have very low cation availability, and Ca^{2+} limits biological processes within infertile Amazonian forests (Cuevas and Medina, 1988).

We suggest that ferns—and particularly older lineages of leptosporangiate ferns—provide a valuable system with which we can both incorporate Ca (and other elements) into terrestrial stoichiometry in a meaningful way, and provide insights to a more fundamental analysis of C-quality. Initially, we became interested in ferns because several species contribute substantially to productivity and nutrient cycling in many Hawaiian forests (Russell et al., 1998). At least some of these ferns differ systematically in foliar chemistry from familiar angiosperms—with remarkably low concentrations of Ca (often <1 mg/g) and Mg, and high concentrations of K and Si (Amatangelo and Vitousek, 2008; Vitousek, 2004). These ferns also decompose more slowly than expected from standard indicators of tissue quality like N, lignin, and polyphenols (Scowcroft, 1997). How widespread are these differences? What controls them? What are their implications, for the many ecosystems where both ferns and angiosperms are abundant? What can we learn from this system that will be applicable to most or all terrestrial ecosystems?

Compound-specific spectral imaging of microorganisms at spatial resolutions approaching 30 nm permits the calculation of C/N, N/Ca, C/P ratios and at the level of individual microorganisms, answers questions such as the trophic level and nutritional plasticity of microbes (Elsser and Hamilton, 2007; Makino et al., 2003). Silicon nitride (Si_3N_4) windows are the preferred X-ray microscope substrate for our experiments at BL 5.3.2 and 11.0.2 at the Advanced Light Source, and at 75 nm thickness, allow STXM for all elements (including N) within range of the Beamlines—by "soft" X-rays, we adopt the convention of referring to all spectroscopic techniques using monochromator-selected energies ~ 100-1200 eV (see Fig. 7.1). STXM uses a lens to produce a demagnified image of a small radiation source, raster-scanning a specimen through the demagnified spot, detecting the radiation which emerges, and using a computer or other device to display the picture. We imaged biofilms developing directly on 75-nm film thickness Si_3N_4 windows (NORCADA; Edmonton, CA) placed in litter bags during the course of 1.5 year-duration greenhouse decomposition experiment. This experiment evaluates controls of decomposition, element dynamics, and microbial communities using manipulative experiments in a greenhouse. We used the litter of six species in this experiment—two older "basal" ferns (*Dicranopteris linearis* and *Cibotium glaucum*), two modern polypod ferns (*Elaphoglossum crassicaule* and *Diplazium sandwichianum*), and two angiosperms (*Metrosideros polymorpha* and *Cheirodendron trigynum*). Litter of the first species in each pair is much lower in N and P than the other, and decomposes about three times more slowly in a common forest plot (Vitousek, 2004). We use a single coarse-textured soil for this experiment, "seeding" it after initial sterilization (with a closed—Gamma source of ^{137}Cs at Stanford's Medical School) with a mixed inoculum of Hawaiian forest floor material collected under all of these species. Litter microcosms are maintained under warm, wet conditions in a greenhouse at Stanford; we utilized time points per substrate, and 5 microcosms per treatment and time. We currently have 24 Si_3N_4-windows (four replicates, embedded in each of six forest litter types): two "basal" ferns, two "polypod" ferns, and two angiosperm tree species.

We now present preliminary STXM data acquired at BL 11.0.2 and 5.3.2 at Berkeley's ALS with Dr. Tolek Tyliszczak on the decomposer-communities associated with two "antipode" species of our tropical litter spectrum: the fast-decomposing tree *Cheirodendron trigynum*, and the ultra-slow decomposing tree fern, *Cibotium glaucum*, both harvested after 90 days.

Author's personal copy

We sought first to directly image the microorganisms on the decomposing plant material as a complement for ongoing RNA-based and enzymatic studies of decomposition on our six vastly differing tropical plant substrates. High-resolution images obtained to date using STXM for such microbial biofilm assemblies (Dynes et al., 2006; Lawrence et al., 2003) relied on imaging thin (50-500 nm thickness) hydrated biofilms, with no sectioning required. The primary elements that we sought to image were the C-1s region (~284.2 eV), the Ca-2s region (~348.4 eV), and the N-1s window (~401 eV). We sought spatially resolved data for bacteria and/or fungal hyphae forming biofilms on the X-ray windows over an area of a few square millimeters, for the purpose of calculating chemical element ratios of C/Ca, N/Ca in the decomposers, for comparison with the plant substrates themselves (using bulk techniques). Recently published data on these plants (Amatangelo and Vitousek, 2008) recorded a 20-40 fold higher N/Ca ratio of angiosperms (e.g. *Cheirodendron*) as compared with basal ferns (e.g. *Cibotium*), depending on the forest soil age at the plants' Hawaiian collection sites. One of our initial hypotheses was that differing nutrient requirements, e.g. for fungi versus bacteria, would be a selection pressure for microorganisms growing on the plant litter itself over long periods of time. The high spatial resolution possible at BL 11.0.2 (with 35 or 40 nm Fresnel zone-plates) provides very clear discrimination between bacterial and fungal structures, and a wealth of internal detail.

One of our first observations from the early part of the litter decomposition experiment relates to the very nature of the decomposer community. As seen in Fig. 7.7A, bacteria dominate the decomposer biofilms on the fast-decomposing tropical tree, *Cheirodendron trigynum*. Imaging of the slow-decomposing tree-fern *Cibotium glaucum* showed a quite different community, with fungal hyphae covering the X-ray window. Contrast in the STXM images arises from the presence of X-ray absorption edges (Fig. 7.7B) for all the important elements in living tissues in the soft X-ray region (100-1200 eV)—and if one centers the spectrum near an edge for a particular element, additional X-ray absorbance features arise from the subtly different electronic environment of the neighboring atoms in covalent bonds. Thus, aliphatic C bonded to C in a waxy aliphatic might absorb at 287 eV, while the same C atom, now bound to a highly electronegative oxygen atom in a polysaccharide ester bond absorbs at 288.6 eV. Though these appear as small energy differences, STXM beamlines typically provide radiation with a center energy good to ± 0.1 eV. The first STXM image represents bacterial cells growing and dividing on the Si_3N_4 windows previously interspersed with fast-decomposing leaves of the tropical tree *Cheirodendron trigynum* (Fig. 7.8). The image has been acquired above the C-edge, at 295 eV. The image to the right is of the same bacterial assemblage, but now acquired at the energy of 288.6 eV, assigned to a 1s- $>$ π^* transition of a carboxyl-C (Boyce et al., 2002). The ragged halo of this latter image we interpret as a polysaccharide-rich sheath forming a cohesive biofilm around the dividing microorganisms, which in the original (protein- and nucleic acid-weighted image) shows very clear cell division plates and endomembrane compartments. The third image in the triptych arises from the Ca-2s image of the very same bacterial assemblage, but tuned to 348.4 eV. Notice first that the intensity of the images is much lower than for the C-images, an effect explained partly by low concentrations of Ca^{2+} in the bacterial biofilm. Also, angular "endplates" apparently associated with recently divided cells can be seen in the Ca-image.

Forest litter derived from a slow-decomposing tree fern *Cibotium glaucum* differed in so far as the STXM slides we have so far examined in detail

Author's personal copy

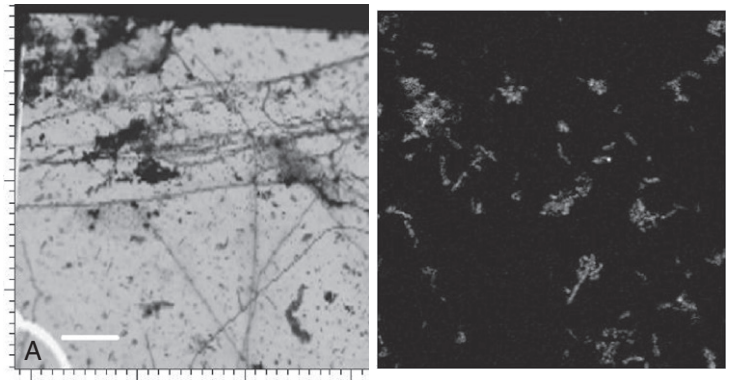

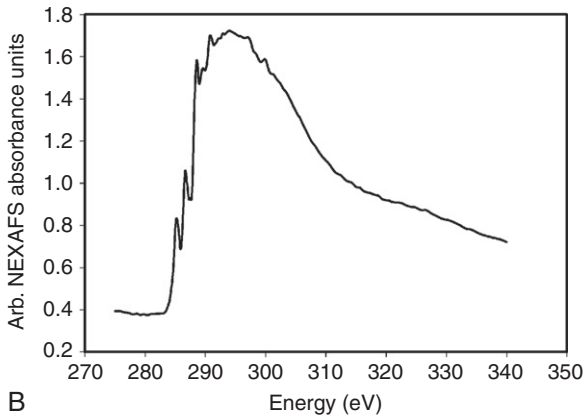

FIGURE 7.7 (A) Overview of the fields covered by Si_3N_4 windows for STXM of 90d-old tropical litter communities. On the left is a negative image taken from microbes colonizing leaf material of the tree fern *Cibotium glaucum*, a slow decomposing species. On the right is the positive image from the leaf material of the tree *Cheirodendron trigynum*, a rapid decomposer (scale bar on the left is for both images = 50 μm). (B) NEXAFS spectrum for the carbon-1s edge of *Cibotium glaucum* litter, showing several near-edge absorption features.

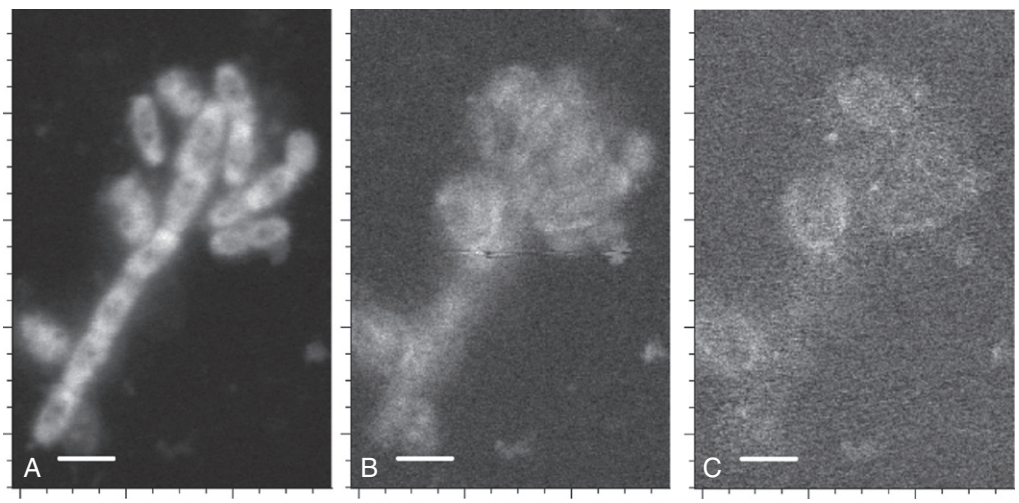

FIGURE 7.8 Matched STXM images of a rapidly dividing group of actinomycetes colonizing litter of the tropical tree *Cheirodenron trigynum*. (A) The C-1s (K-edge) image centered at 288.3 eV. (B) C-1s image centered at 286.6 eV. Notice the larger spatial extent of this image than the previous C band. (C) Ca-2s (L-edge) image at 348.4 eV. Especially Ca-rich angular end-caps appear on a subset of the microbes, perhaps associated with the nascent polysaccharide-rich biofilm, or an indication of recent cell-division (scale bar for all images = 1 μm).

Author's personal copy

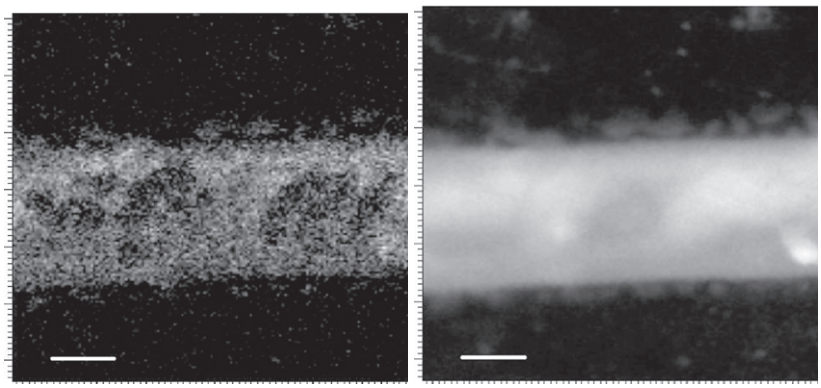

FIGURE 7.9 Matched STXM images of fungal hyphae associated with litter of the tree fern *Cibotium glaucum*. On the left is the Ca-L edge image at 348.4 eV, while the corresponding C-1s spectrum at 295 eV (above the K-edge) is shown on the right (scale bar for both images = 1 μm).

have been overrun with fungal hyphae, consistent with bacterial/basidiomycete abundances derived from both DNA extraction and lignin peroxidase enzyme activities measured directly from the litter (Amatangelo and Raab, unpublished data). In Fig. 7.9, we have two high-resolution STXM images of a portion of the hyphal network seen at Ca energies (348.4.4 eV) and C (295 eV, post-edge). Based on the similarities in the exposure times for the bacterial and fungal images, we can see immediately that the initial expectation—that fungal tissues would be enriched in Ca relative to the peptidoglycan walls of bacteria—is confirmed.

STXM may provide insights on sink-source relationships between plants, mycorrhizal fungi, and other rhizosphere organisms. Determining whether endophytic fungi serve parasitic or mutualistic roles is sometimes difficult; visualizing concentration gradients of C, N, and P along roots and fungal hyphae could help address this question. Another topic of major interest in the mycorrhizosphere is the production and fate of glomalin. Glomalin contributes greatly to the stability of soil aggregates and is a major component of soil OM, but its quantification is made difficult by rapid transformation in the soil (Rillig and Steinberg, 2002). This glycoprotein is produced in large amounts by AM, and so prospects are good for its detection by STXM, and as we have demonstrated, potentially in the thermal IR region.

Investigating the effects of roots on the activity and composition of the rhizosphere microbial community will require the high resolution, chemically specific information provided by STXM to be combined with species-specific molecular probes, so that chemical and microbial diversity data can be combined. STXM and confocal laser scanning microscopy (CLSM) have been combined in a study of macromolecules within bacterial biofilms (Lawrence et al., 2003). A similar approach could be used in which STXM is combined with fluorescent *in situ* hybridization (FISH), in which labeled oligonucleotides or antibodies are used to probe specific microbial taxa (Hahn et al., 1992). Rather than using a combined microscopy technique, an alternative is to use molecular probes labeled with gold, or some other high-Z element easily detectable with STXM, and simultaneously image specific groups of microbes and their chemical surroundings (Gerard et al., 2005). The challenge to such an approach lies in preserving the chemical and spatial integrity of the environment while fixing and probing the sample. Another challenge in

Author's personal copy

studying the activities and composition of rhizosphere microbial communities is that of determining the rates of processes occurring at fine spatial scales. In some cases, rates of uptake, transformation or secretion may be inferred from observed concentration gradients around the root or microcolony, provided sufficient knowledge of diffusion rates exists for the system. However, more generally, timed incubations need to be performed. Toner et al. (2005) studied Mn oxidation over time in a liquid culture of *P. putida* by removing samples, sealing them within Si_3N_4 "sandwiches" and immediately observing with STXM. Likewise, Benzerara et al. (2004) probed different Ca-based mineral phases attendant calcification in culture suspensions of the model bacterium *Caulobacter crescentus* dried onto Si_3N_4 windows. Constructing chambers in which rhizosphere processes can proceed, and from which minimally disturbed STXM-ready samples can be prepared, will require creativity and care.

10. CONCLUSIONS

At two energy "endpoints" of the EM spectrum accessible to synchrotron biologists (IR radiation and soft X-rays), we have found experimental methods providing unique opportunities to observe processes and test hypotheses essential to understanding plant-soil-microbe interactions. Availability of IR synchrotron beamlines will continue to expand worldwide, and we hope that plant and microbial biologists will incorporate the type of spectral data presented in this chapter as just one of a legion of "-omics" methods. Considering the shear flux of C through belowground ecosystems annually (and how poorly constrained they are in many regions), synchrotrons must continue to demand the attention of ecologists and plant breeders. We have no doubt that the precise accounting of elemental ratios within decomposer communities (poorly accessible experimentally compared to primary producers) will uncover new chokepoints for determining the ultimate suite of limiting nutrients to terrestrial plants. Culture-independent methods for the identification of microorganisms will likewise benefit from high spatial resolution studies of pure and mixed biofilms, in so far as the chemical transformations of C, N, P (and a host of other important elements in the periodic table) continue to underlie the functioning of the Planet.

ACKNOWLEDGMENTS

We thank Drs. Michael C. Martin (BL 1.4.3, 1.4.4) and Tolek Tyliszczak (BL 11.0.2, 5.3.2) of the Advanced Light Source, Berkeley CA for their unwavering friendship and support over the last decade of our involvement with synchrotron biology. We thank Dr. Kathryn L. Amatangelo (University of Wisconsin) for sharing prepublication data with us, and our friend/colleague Peter M. Vitousek for providing 'ohana. Support from the National Science Foundation is gratefully acknowledged, esp. NSF DEB-0516491 to Stanford, NSF OPP-0421588 to SDSU, and early exploratory funding from NASA to the University of Colorado. The Advanced Light Source is supported by the Director, Office of Science, Office of Basic Energy Sciences, of the U.S. Department of Energy under Contract No. DE-AC02-05CH11231.

References

Ae, N., Arihara, J., Okada, K., Yoshihara, T., Johnasen, C., 1990. Phosphorus uptake by pigeon pea and its role in cropping systems of the Indian subcontinent. Science 248, 477–480.

Amatangelo, K.L., Vitousek, P.M., 2008. Stoichiometry of ferns in Hawaii: implications for nutrient cycling. Oecologia 157 (4), 619–627.

Bais, H.P., Weir, T.L., Perry, L.G., Gilroy, S., Vivanco, J.M., 2006. The role of root exudates in rhizosphere interactions with plants and other organisms. Annu. Rev. Plant Biol. 57, 233–266.

Author's personal copy

Banfield, J.F., Barker, W.W., Welch, S.A., Taunton, A., 1999. Biological impact on mineral dissolution: application of the lichen model to understanding mineral weathering in the rhizosphere. Proc. Natl. Acad. Sci. 96, 3404–3411.

Bañuelos, G., Terry, N., LeDuc, D., Pilon-Smits, E.A.H., Mackey, B., 2004. Field trial of transgenic Indian mustard plants shows enhanced phytoremediation of selenium-contaminated soil. Environ. Sci. Techol. 39, 1771–1777.

Barnard, A.M.L., Bowden, S.D., Burr, T., 2007. Quorum sensing, virulence and secondary metabolite production in plant soft-rotting bacteria. Philos. Trans. R. Soc. B Biol. Sci. 362, 1165–1183.

Benzerara, K., Yoon, T.H., Tyliszczak, T., Constanz, B., Spormann, A.M., Brown, G.E., 2004. Scanning transmission X-ray microscopy study of microbial calcification. Geobiology 2, 249–259.

Benzerara, K., Yoon, T.H., Menguy, N., Tyliszczak, T., Brown, G.E., 2005. Nanoscale environments associated with bioweathering of a Mg-Fe-pyroxene. Proc. Natl. Acad. Sci. 102, 979–982.

Bertin, C., Weston, L.A., Huang, T., Jander, G., Owens, T., Meinwald, J., et al., 2007. Grass roots chemistry: meta-Tyrosine, an herbicidal nonprotein amino acid. Proc. Natl. Acad. Sci. 104, 16964–16969.

Blanchar, R.W., Lipton, D.S., 1986. The pe and pH in alfalfa seedling rhizospheres. Agron. J. 78, 216–218.

Blum, J.D., Klaue, A.D., Nezat, C.A., Driscoll, C.T., Johnson, C.E., Siccama, T.G., et al., 2002. Mycorrhizal weathering of apatite as an important calcium source in base-poor forest ecosystems. Nature 417, 729–731.

Boyce, C.K., Cody, G.D., Feser, M., Jacobsen, C., Knoll, A.H., Wirick, S., et al., 2002. Organic chemical differentiation within fossil plant cell walls detected with X-ray spectromicroscopy. Geology 30, 1039–1042.

Buol, S.W., Hole, F.D., McCracken, R.J., 1973. Soil Genesis and Classification. Iowa State University Press, Ames.

Cardon, Z.G., Gage, D.J., 2006. Resource exchange in the rhizosphere: molecular tools and the microbial perspective. Annu. Rev. Ecol. Evol. Syst. 37, 459–488.

Carr, G.L., 1999. High-resolution microspectroscopy and sub-nanosecond time-resolved spectroscopy with the synchrotron IR source. Vib. Spectrosc. 19, 53–60.

Carr, G.L., Hanfland, M., Williams, G.P., 1995. MidIR beamline at the National Synchrotron Light Source port U2B. Rev. Sci. Instrum. 66, 1643–1645.

Chadwick, O.A., Derry, L., Vitousek, P.M., Huebert, B.J., Hedin, L.O., 1999. Changing sources of nutrients during four million years of ecosystem development. Nature 397, 491–497.

Chandran, D., Sharopova, N., vanDenBosch, K.A., Garvin, D.F., Samac, D.A., 2008. Physiological and molecular characterization of aluminum resistance in Medicago truncatula. BMC Plant Biol. 8, 89.

Chen, X., Schauder, S., Potier, N., Van Dorsselaer, A., Pelczer, I., Bassler, B.L., et al., 2002. Structural identification of a bacterial quorum-sensing signal containing boron. Nature 415, 545–549.

Clarholm, M., 1985. Interactions of bacteria, protozoa and plants leading to mineralization of soil nitrogen. Soil Biol. Biochem. 17, 181–187.

Clifford, S.C., Arndt, S.K., Popp, M., Jones, H.G., 2002. Mucilages and polysaccharides in *Ziziphus* species (Rhamnaceae): localization, composition and physiological roles during drought-stress. J. Exp. Bot. 53, 131–138.

Coimbra, M.A., Barros, A., Barros, M., Rutledge, D.N., Delgadillo, I., 1998. Multivariate analysis of uronic acid and neutral sugars in whole pectic samples by FT-IR spectroscopy. Carbohyd. Polym. 37, 241–248.

Cuevas, E., Medina, E., 1988. Nutrient dynamics within Amazonian forests. II. Fine root growth, nutrient availability, and leaf litter decomposition. Oecologia 76, 222–235.

Darrah, P.R., 1991. Models of the rhizosphere. 2. A quasi 3-dimensional simulation of the microbial-population dynamics around a growing root releasing soluble exudates. Plant Soil 138, 147–158.

Darrah, P.R., Jones, D.L., Kirk, G.J.D., Roose, T., 2006. Modeling the rhizosphere: a review of methods for 'upscaling' to the whole-plant scale. Eur. J. Soil Sci. 57, 13–25.

Daufresne, T., Loreau, M., 2001. Plant-herbivore interactions and ecological stoichiometry: when do herbivores determine plant nutrient limitation? Ecol. Lett. 4, 196–206.

Dinkelaker, B., Röhmeld, V., Marschner, H., 1989. Citric acid excretion and precipitation of calcium citrate in the rhizosphere of white lupin (*Lupinus albus* L.). Plant Cell Environ. 12, 285–292.

Dufey, J.E., Braun, R., 1986. Cation exchange capacity of roots: titration, sum of exchangeable cations, copper adsorption. J. Plant Nutr. 9, 1147–1155.

Dynes, J.J., Tyliszczak, T., Araki, T., Lawrence, J.R., Swerhone, G.D.W., Leppard, G.G., et al., 2006. Speciation and quantitative mapping of metal species in microbial biofilms using scanning transmission X-ray microscopy. Environ. Sci. Technol. 40, 1556–1565.

Elsser, J.J., Hamilton, A., 2007. Stoichiometry and the new biology: the future is now. PLoS Biol. 5, 1403–1405.

Faber, B.A., Zasoski, R.J., Munns, D.N., Shackel, K., 1991. A method for measuring the hyphal nutrient and water uptake in mycorrhizal plants. Can. J. Bot. 69, 87–94.

Fan, T.W.M., Lane, A.N., Pedler, J., Crowley, D., Higashi, R. M., 1997. Comprehensive analysis of organic ligands in whole root exudates using nuclear magnetic resonance and gas chromatography-mass spectrometry. Anal. Biochem. 251, 57–68.

Farmer, V.C, 1974. The IR Spectra of Minerals. Mineralogical Society, London UK.

Author's personal copy

Feeney, D.S., Crawford, J.W., Daniell, T., Hallettt, P.D., Nunan, N., Ritz, K., et al., 2006. Three-dimensional microorganization of the soil-root-microbe system. Microb. Ecol. 52, 151–158.

Fiehn, O., Kopka, J., Dormann, P., Altmann, T., Trethewey, R.N., Willmitzer, L., 2000. Metabolite profiling for plant functional genomics. Nat. Biotech. 18, 1157–1161.

Finzi, A.C., Norby, R.J., Calfapietra, C., 2007. Increases in nitrogen uptake rather than nitrogen-use efficiency support higher rates of temperate forest productivity under elevated CO_2. Proc. Natl. Acad. Sci. 104, 14014–14019.

Fredeen, A.L., Rao, I.M., Terry, N., 1989. Influence of phosphorus-nutrition on growth and Carbon partitioning in Glycine max L. Plant Physiol. 89, 225–230.

Gerard, E., Guyot, F., Philippot, P., Lopez-Garcia, P., 2005. Fluorescence *in situ* hybridisation coupled to ultra small immunogold detection to identify prokaryotic cells using transmission and scanning electron microscopy. J. Microbiol. Methods 63, 20–28.

Ghosh, D., Roy, K., Williamson, K.E., White, D.C., Wommack, K.E., Sublette, K.L., et al., 2008. Prevalence of lysogeny among soil bacteria and presence of 16S rRNA and *trzN* genes in viral-community DNA. Appl. Environ. Microbiol. 74, 495–502.

Gierlinger, N., Schwanninger, M., 2007. The potential of Raman microscopy and Raman imaging in plant research. Spectroscopy 21, 69–89.

Gill, R.A., Jackson, R.B., 2000. Global patterns of root turnover for terrestrial ecosystems. New Phytol. 147, 13–31.

Hahn, D., Amann, R.I., Ludwig, W., Akkermans, A.D.L., Schleifer, K.H., 1992. Detection of microorganisms in soil after *in situ* hybridization with rRNA-targeted, fluorescently labelled oligonucleotides. J. Gen. Microbiol. 138, 879–887.

Herman, D.J., Johnson, K.K., Jaeger, C.H., 2006. Root influence on nitrogen mineralization and nitrification in *Avena barbata* rhizosphere soil. Soil Sci. Soc. Am. J. 70, 1504–1511.

Hickok, L.G., Warne, T.R., Fribourg, R.S., 1995. The biology of the fern *Ceratopteris* and its use as a model system. Int. J. Plant Sci. 156, 332–345.

Hiltner, L., 1904. Über neuere Erfahrungen und probleme auf dem gebiete der Bodenbakteriologie unter besonderer Berücksichtigung der gründüngung und Brache. Arbeiten der Deitschen Landwirtschaftlichen Gesellschaft 98, 59–78.

Hinsinger, P., Gobran, G.R., Gregory, P.J., Wenzel, W.W., 2005. Rhizosphere geometry and heterogeneity arising from root mediated physical and chemical processes. New Phytol. 168, 293–303.

Hirai, M.Y., Yano, M., Goodenowe, D.B., Kanyaka, S., Kimura, T., Awazuhara, M., et al., 2004. Integration of transcriptomics and metabolomics for understanding the global responses of nutritional stresses in *Arabidopsis thaliana*. Proc. Natl. Acad. Sci. 101, 10205–10210.

Hitchcock, A.P., Morin, C., Zhang, X., Araki, T., Dynes, J., Stover, H., et al., 2005. Soft X-ray spectromicroscopy of biological and synthetic polymer systems. J. Electron Spectros. Relat. Phenomena 144–147, 259–269.

Holtsmark, I., Eijsink, V.G.H., Brurberg, M.B., 2007. Bacteriocins from plant pathogenic bacteria. FEMS Microbiol. Lett. 280, 1–7.

Hückelhoven, R., 2007. Transport and secretion in plant-microbe interactions. Curr. Opin. Plant Biol. 10, 573–579.

Hungate, B.A., Holland, E.A., Jackson, R.B., Chapin, F.S., Mooney, H.A., Field, C.B., 1997. The fate of carbon in grasslands under carbon dioxide enrichment. Nature 388, 576–579.

Ingham, R.E., Trofymow, J.A., Ames, R.N., Hunt, H.W., Morley, C.R., Moore, J.C., et al., 1986. Trophic interactions and nitrogen cycling in a semi-arid grassland. I. Seasonal dynamics of the natural populations, their interactions and effects on nitrogen cycling. J. Appl. Ecol. 23, 597–614.

Jacobsen, C., Williams, S., Anderson, E., Browne, M.T., Buckley, C.J., Kern, D., et al., 1991. Diffraction-limited imaging in a scanning transmission x-ray microscope. Opt. Commun. 86, 351–364.

Jacobsen, C., Wirick, S., Flynn, G., Zimba, C., 2000. Soft x-ray spectroscopy from image sequences with sub-100 nm spatial resolution. J. Microsc. 197, 86–104.

Jamin, N., Dumas, P., Moncuitt, J., Fridman, W.H., Teillaud, J.L., Carr, G.L., et al., 1998. Highly resolved chemical imaging of living cells by using synchrotron IR microspectrometry. Proc. Natl. Acad. Sci. 95, 4837–4840.

Jarvis, M.C., 1984. Structure and properties of pectin gels in plant cell walls. Plant Cell Environ. 7, 153–164.

Jones, M.D., Durall, D.M., Tinker, P.B., 1990. Phosphorus relationships and production of extramatrical hyphae by two types of willow ectomycorrhizas at different soil-phosphorus levels. New Phytol. 115, 259–267.

Kacurakova, M., Petrakova, E., Ebringerova, A., 1990. IR spectra of the positional isomers of the methyl xylobiosides in the "anomeric region." Carbohydr. Res. 207, 121–125.

Kacurakova, M., Capek, P., Sainkova, V., Wellner, N., Ebringerova, A., 2000. FT-IR study of plant cell wall model compounds: pectic polysaccharides and hemicelluloses. Carbohydr. Polym. 43, 195–203.

Kaminsky, S., Jilkin, K., Szeghalmi, A., Gough, K., 2008. High spatial resolution analysis of fungal cell biochemistry: bridging the analytical gap using synchrotron FTIR spectroscopy. FEMS Microbiol. Lett. 284, 1–8.

Author's personal copy

Katznelson, H., Rouatt, J.W., Peterson, E.A., 1962. The rhizosphere effect of mycorrhizal and non-mycorrhizal roots of yellow birch seedlings. Can. J. Bot. 40, 377–382.

Kinyangi, J., Solomon, D., Liang, B., Lerotic, M., Wirick, S., Lehmann, J., 2006. Nanoscale biogeocomplexity of the organomineral assemblage in soil: application of STX microscopy and C-1s NEXAFS spectroscopy. Soil Sci. Soc. Am. J. 70, 1708–1718.

Kochian, L.V., 1995. Cellular mechanisms of Aluminum toxicity and resistance in plants. Annu. Rev. Plant Physiol. Plant Mol. Biol. 46, 237–260.

Kochian, L.V., Hoekenga, O.A., Pińeros, M.A., 2004. How do crop plants tolerate acid soils ? Mechanisms of aluminum tolerance and phosphorus efficiency. Annu. Rev. Plant Biol. 55, 459–493.

Kono, H., Nakato, T., Nakashima, S., Kato, K., 2005. *Lygodium japonicum* fern accumulates copper in cell wall pectin. J. Exp. Bot. 56, 1923–1931.

Kuzyakov, Y., 2002. Review: factors affecting rhizosphere priming effects. J. Plant Nutr. Soil Sci. 165, 382.

Kuzyakov, Y., Leinweber, P., Sapronov, D., Eckhardt, K.U., 2003. Qualitative assessment of rhizodeposits in non-sterile soil by analytical pyrolysis. J. Plant Nutr. Soil Sci. 166, 719–723.

Lambrecht, M., Okon, Y., Vande Broek, A., Vanderleyden, J., 2000. Indole-3-acetic acid: a reciprocal signaling molecule in bacteria-plant interactions. Trends Microbiol. 8, 298.

Lawrence, J.R., Swerhone, G.D.W., Leppard, G.G., Araki, T., Zhang, X., West, M.M., et al., 2003. Scanning transmission X-ray, laser scanning, and transmission electron microscopy mapping of the exopolymeric matrix of microbial biofilms. Appl. Environ. Microbiol. 69, 5543–5554.

Levenson, E., Lerch, P., Martin, M.C., 2008. Spatial resolution limits for synchrotron-based IR spectromicroscopy. Infrared Phys. Technol. 51, 413–416.

Likens, G.E., Driscoll, C.T., Buso, D.C., Siccama, T.G., Johnson, C.E., Lovett, G.M., et al., 1998. The biogeochemistry of calcium at Hubbard Brook. Biogeochemistry 41, 89–173.

Lipson, D.A., Schmidt, S.K., Monson, R.K., 1999. Links between microbial population dynamics and N availability in an alpine ecosystem. Ecology 80, 1623–1631.

Lipson, D.A., Wilson, R.A., Oechel, W.C., 2005. Effects of elevated atmospheric CO_2 on soil microbial biomass, activity and diversity in a chaparral ecosystem. Appl. Environ. Microbiol. 71, 8573–8580.

Lipton, D.S., Blanchar, R.W., Blevins, D.G., 1987. Citrate, malate, and succinate concentration in exudates from P-sufficient and P-stressed *Medicago sativa* L. seedlings. Plant Physiol. 85, 315–317.

Loyola-Vargas, V.M., Broeckling, C.D., Badri, D., Vivanco, J.M., 2007. Effect of transporters on the secretion of phytochemicals by the roots of *Arabidopsis thaliana*. Planta 225, 301–310.

Mahall, B.E., Callaway, R.M., 1991. Root communication among desert shrubs. Proc. Natl. Acad. Sci. 88, 874–876.

Makino, W., Cotner, J.B., Sterner, R.W., Elser, J.J., 2003. Are bacteria more like plants or animals? Growth rate and resource dependence of bacterial C:N:P stoichiometry. Funct. Ecol. 17, 121–130.

Makjanic, J., Vis, R.D., Groneman, A.F., Gommers, F.J., Henstra, S., 1988. Investigation of the P and S distributions of *Tagetes patula* L. using micro-PIXE. J. Exp. Bot. 39, 1523–1528.

Mancosky, D.G., Lucia, L.A., Nanko, H., Wirick, S., Rudie, A.W., Braun, R., 2005. Novel visualization studies of lignocellulosic oxidation chemistry by application of C-near edge X-ray absorption fine structure spectroscopy. Cellulose 12, 35–41.

Marschner, H., Rohmeld, V., Ossenbergneuhaus, H., 1982. Rapid method for measuring changes in pH and reducing processes along roots of intact plants. Z. Pflanzenphysiol.,^{L} 105, 407–416.

Martin, M.C., McKinney, W.R., 1998. The first synchrotron IR beamlines at the Advanced Light Source: microspectroscopy and fast timing. Proc. Mater. Res. Soc. 524, 11.

Martin, M.C., Tsvetkova, N.M., Crowe, J.H., McKinney, W. R., 2001. Negligible sample heating from synchrotron IR beam. Appl. Spectrosc. 55, 111–113.

Mathesius, U., Mulders, S., Gao, M., Teplitski, M., Caetano-Anolles, G., Rolfe, B.G., et al., 2003. Extensive and specific responses of a eukaryote to bacterial quorum sensing signals. Proc. Natl. Acad. Sci. 100, 1444–1449.

Mathlouthi, M., Koenig, J.L., 1986. Vibrational spectra of carbohydrates. Adv. Carbohydr. Chem. Biochem. 44, 1–66.

McLaughlin, S.B., Wimmer, S.R., 1999. *Tansley Review #140*. Calcium physiology and terrestrial ecosystem processes. New Phytol. 142, 373–417.

Merk, S., Blume, A., Riederer, M., 1998. Phase behavior and crystallinity of plant cuticular waxes studies by Fourier transform IR spectroscopy. Planta 204, 44–53.

Morris, C.E., Monier, J.M., 2003. The ecological significance of biofilm formation by plant-associated bacteria. Annu. Rev. Phytopathol. 41, 429–453.

Morris, E.R., Powell, D.A., Gidley, M.J., Rees, D.A., 1982. Conformations and interactions of pectins. I. Polymorphism between gel and solid states of calcium polygalacturonate. J. Mol. Biol. 155, 507–516.

Muller, R., Nilsson, L., Krintel, C., Nielsen, T.H., 2004. Gene expression during recovery from phosphate starvation in roots and shoots of *Arabidopsis thaliana*. Physiol. Plant 122, 233–243.

Author's personal copy

Myrold, D.D., 1994. *Frankia* and the actinorhizal symbiosis. In: Weaver, R.W., Angle, S., Bottomley, P.J. (Eds.), Methods of Soil Analysis, Part 2. Microbiological and Biochemical Properties. Soil Sci. Soc. Am., Madison, WI, pp. 291–328.

Peters, N.K., Long, S.R., 1988. Alfalfa root exudates and compounds which promote or inhibit induction of *Rhizobium meliloti* nodulation genes. Plant Physiol. 88, 396–400.

Phillips, R.P., Fahey, T.J., 2006. Tree species and mycorrhizal associations influence the magnitude of rhizosphere effects. Ecology 87 (5), 1302–1313.

Pieterse, C.M.J., Dicke, M., 2007. Plant interactions with microbes and insects: from molecular mechanisms to ecology. Trends Plant Sci. 12, 564–569.

Polonenko, D.R., Mayfield, C.I., 1979. A direct observation technique for studies on rhizoplane and rhizosphere colonization. Plant Soil 51, 405–420.

Powell, C.L., Bagyaraj, J., 1984. VA Mycorrhiza. CRC Press, Boca Raton, FL.

Raab, T.K., Martin, M.C., 2001. Visualizing rhizosphere chemistry of legumes with mid-IR synchrotron radiation. Planta 213 (6), 881–887.

Raab, T.K., Vogel, J.P., 2004. Ecological and agricultural applications of synchrotron IR microscopy. IR Phys. Technol. 45, 393–402.

Raab, T.K., Lipson, D.A., Monson, R.K., 1999. Soil amino acid utilization among species of the Cyperaceae: plant and soil processes. Ecology 80, 2408–2419.

Raab, T.K., Amatangelo, K.A., Vitousek, P.M., 2010. Biochemical diversity among Hawaiian ferns, tree ferns and angiosperms: implications for life-forms and nutrient retention. J. Ecol. (in press).

Rao, I.M., Borrero, V., Ricaurte, J., Garcia, R., 1999. Adaptive attributes of tropical forage species to acid soils. V. Differences in phosphorus acquisition from less available inorganic and organic sources of phosphate. J. Plant Nutr. 22, 1175–1196.

Rao, I.M., Ziegler, R.S., Vera, R., Sarkarung, S., 1993. Selection and breeding for acid-soil tolerance in crops. Bioscience 43, 454–465.

Raynaud, X., Lata, J.C., Leadley, P.W., 2006. Soil microbial loop and nutrient uptake by plants: a test using a coupled C:N model of plant-microbial interactions. Plant Soil 287, 95–116.

Raynaud, X., Jaillard, B., Leadley, P.W., 2008. Plants may alter competition by modifying nutrient bioavailability in rhizosphere: a modeling approach. Am. Nat. 171, 44–58.

Read, D.J., Boyd, R., 1986. Water relations of mycorrhizal fungi and their host plants. In: Ayres, P.G., Boddy, L. (Eds.), British Mycological Society Symposium, 11. Water, Fungi And Plants. Lancaster, England, Apr. 1985. Cambridge University Press, Cambridge, England, pp. 287–304 .

Read, D.J., Duckett, J.G., Francis, R., Ligrone, R., Russell, A., 2000. Symbiotic fungal associations in 'lower' land plants. Philos. Trans. R. Soc. Lond. B 355, 815–831.

Reffner, J.A., Martoglio, P.A., Williams, G.P., 1995. Fourier transform IR microscopical analysis with synchrotron radiation: the microscope optics and system performance. Rev. Sci. Instrum. 66, 1298–1302.

Rillig, M.C., Steinberg, P.D., 2002. Glomalin production by an arbuscular mycorrhizal fungus: a mechanism of habitat modification? Soil Biol. Biochem. 34, 1371–1374.

Roelofs, R.F.R., Rengel, Z., Cawthray, G.R., Dixon, K.W., Lambers, H., 2001. Exudation of carboxylates in Australian Proteaceae: chemical composition. Plant Cell Environ. 24, 891–903.

Rousseau, J.V.D., Sylvia, D.M., Fox, A.J., 1994. Contribution of ectomycorrhiza to the potential nutrient-absorbing surface of pine. New Phytol. 128, 639–644.

Russell, A.E., Raich, J.W., Vitousek, P.M., 1998. The ecology of the climbing fern Dicranopteris linearis on windward Mauna Loa. Hawaii. J. Ecol. 86. 765–779.

Ryan, R.P., Germaine, K., Franks, A., Ryan, D.J., Dowling, D.N., 2008. Bacterial endophytes: recent developments and applications. FEMS Microbiol. Lett. 278, 1–9.

Saj, S., Mikola, J., Ekelund, F., 2007. Root-induced decomposer growth and plant N uptake are not positively associated among a set of grassland plants. Appl. Soil Ecol. 37, 215–222.

Sanchez, P.A., 2002. Soil fertility and hunger in Africa. Science 295, 2019–2020.

Schmidt, S.K., Ley, R.E., 1999. Microbial competition and soil structure limit the expression of allelochemicals in nature. In: Inderjit, D.K.M.M., Foy, C.L. (Eds.), Principles and Practices in Plant Ecology: Allelochemical Interactions. CRC Press, Orlando, FL.

Schmidt, S.K., Lipson, D.A., Raab, T.K., 2000. Effects of willows (*Salix brachycarpa*) on populations of salicylate-mineralizing microorganisms in alpine Soils. J. Chem. Ecol. 26, 2049–2057.

Schumacher, M., Christl, I., Scheinost, A.C., Jacobsen, C., Kretzschmar, R., 2005. Chemical heterogeneity of organic soil colloids investigated by scanning transmission X-ray microscopy and C-1s NEXAFS microspectroscopy. Environ. Sci. Technol. 39, 9094–9100.

Scowcroft, P.G., 1997. Mass and nutrient dynamics of decaying litter from *Passiflora mollissima* and selected native species in a Hawaiian montane rainforest. J. Trop. Ecol. 13, 539–558.

Author's personal copy

Singh, J.S., Raghunbanshi, A.S., Singh, R.S., Srivastava, S.C., 1989. Microbial biomass acts as a source of plant nutrients in dry tropical forest and savanna. Nature 338, 499–500.

Smith, A.R., Pryer, K.M., Schuettpelz, E., Korall, P., Schneider, H., Wolf, P.G., 2006. A classification of ferns. Taxon 55, 705–731.

Somers, E., Vanderleyden, J., Srinivasan, M., 2004. Rhizosphere bacterial signalling: a love parade beneath our feet. Crit. Rev. Microbiol. 30, 205–240.

Sposito, G.S., 1989. The Chemistry of Soils. Oxford University Press, Oxford, UK.

Steeves, T.A., Sussex, I.M., 1989. Patterns in Plant Development, second ed Cambridge University Press, Cambridge, UK.

Stein, M., Dittgen, J., Sanchez-Rodriguez, C., Hou, B.H., Molina, A., Schulze-Lefert, P., et al., 2006. Arabidopsis PEN3/PDR8, an ATP binding cassette transporter, contributes to nonhost resistance to inappropriate pathogens that enter by direct penetration. Plant Cell 18, 731–746.

Strain, E., Hass, B., Banks, J.A., 2001. Characterization of mutations that feminize gametophytes of the fern *Ceratopteris*. Genetics 159, 1271–1281.

Sumner, J., 2000. The Natural History of Medicinal Plants. Timber Press, Portland, OR.

Synytsya, A., Copikova, J., Matejka, P., Machovic, V., 2003. Fourier transform Raman and IR spectroscopy of pectins. Carbohydr. Polym. 54, 97–106.

Teplitski, M., Robinson, J.B., Bauer, W.D., 2000. Plants secrete substances that mimic bacterial N-acyl homoserine lactone signal activities and affect population density-dependent behaviors in associated bacteria. Mol. Plant Microbe Interact. 13, 637.

Toner, B., Fakra, S., Villalobos, M., Warwick, T., Sposito, G., 2005. Spatially-resolved characterization of biogenic manganese Oxide production within a bacterial biofilm. Appl. Environ. Microbiol. 71, 1300–1310.

van der Heijden, M.G.A., Bardgett, R.D., van Straalen, N. M., 2008. The unseen majority: soil microbes as drivers of plant diversity and productivity in terrestrial ecosystems. Ecol. Lett. 11, 296–310.

Vinale, F., Sivasithamparam, K., Ghisalberti, E.L., Marra, R., Woo, S.L., Lorito, M., 2008. Trichoderma–plant–pathogen interactions. Soil Biol. Biochem. 40, 1–10.

Vitousek, P.M., 2004. Nutrient Cycling and Limitation: Hawai'i as a Model System. Princeton University Press, Princeton, NJ.

Vitousek, P.M., Howarth, R.W., 1991. Nitrogen limitation on land and in the sea: how can it occur? Biogeochemistry 13, 87–115.

Vogel, J.P., Raab, T.K., Somerville, C.R., Somerville, S.C., 2004. Mutations in *PMR5* result in powdery mildew resistance and altered cell wall composition. Plant J. 40, 968–978.

Walker, L.R., Boneta, W., 1995. Plant and soil responses to fire on a fern-covered landslide in Puerto Rico. J. Trop. Ecol. 11, 473–479.

Wallander, H., Pallon, J., 2005. Temporal changes in the elemental composition of *Rhizopogon* rhizomorphs during colonization of patches with fresh organic matter or acid-washed sand. Mycologia 97, 295–303.

Wan, J., Tyliszczak, T., Tokunaga, T.K., 2007. Organic carbon distribution, speciation, and elemental correlations within soil microaggregates: applications of STXM and NEXAFS spectroscopy. Geochim. Cosmochim. Acta 71, 5439–5449.

Watanabe, T., Misawa, S., Hiradate, S., Osaki, M., 2008. Characterization of root mucilage from *Melastoma mabrathicum*, with emphasis on its roles in aluminum accumulation. New Phytol. 178, 581–590.

Welch, S.A., Barker, W.W., Banfield, J.F., 1999. Microbial extracellular polysaccharides and plagioclase dissolution. Geochim. Cosmochim. Acta 63, 1405–1419.

Wetzel, D.L., 2002. A new approach to the problem of dispersive windows in IR microspectroscopy. Vib. Spectrosc. 29, 291–297.

Wetzel, D.L., Reffner, J.A., 1993. Using spatially resolved Fourier-transform infrared microbeam spectroscopy to examine the microstructure of wheat kernels. Cereal Food. World 38, 9–20.

Willats, W.G.T., Orfila, C., Limberg, G., Buchholt, H.C., van Alebeek, G.J.W.M., Voragen, A.G.J., et al., 2001. Modulation of the degree and pattern of methyl-esterification of pectin homogalacturonan in plant cell walls. J. Biol. Chem. 276, 19404–19413.

Williams, P., 2007. Quorum sensing, communication and cross-kingdom signalling in the bacterial world. Microbiology 153, 3923–3938.

Yaci, Y., Heyraud, A., Barakat, M., Heulin, T., 2005. Isolation and identification of an EPS_producing *Rhizobium* strain from arid soil (Algeria): characterization of its EPS and the effect of inoculation on wheat rhizosphere soil structure. Res. Microbiol. 156, 522–531.

Yoder, J.I., 2001. Host-plant recognition by parasitic Schrophulariaceae. Curr. Opin. Biol. Plant 4, 259–264.

Yu, P., 2007. Microlocalization and digestion-resistant aromatic lignin and cellulosic compounds in feeds at cellular and subcellular levels: a novel approach. J. Anim. Feed Sci. 16, 505–525.

Yu, P.Q., McKinnon, J.J., Christensen, C.R., Christensen, D.A., Marinkovic, N.S., Miller, L.M., 2003. Chemical imaging of microstructures of plant tissues within cellular dimension using synchrotron IR microspectroscopy. J. Agric. Food Chem. 51, 6062–6067.

Author's personal copy

Yuan, Z.C., Edlind, M.P., Liu, P., Saenkham, P., Banta, L.M., Wise, A.A., et al., 2007. The plant signal salicylic acid shuts down expression of the *vir* regulon and activates quormone-quenching genes in *Agrobacterium*. Proc. Natl. Acad. Sci. 104, 11790–11795.

Zeier, J., Schreiber, L., 1999. Fourier transform infrared-spectroscopic characterisation of isolated endodermal cell walls from plant roots: chemical nature in relation to anatomical development. Planta 209, 537–542.